HISTORICAL BIOLOGY
https://doi.org/10.1080/08912963.2025.2568707

Taylor & Francis
Taylor & Francis Group

RESEARCH ARTICLE

Eternauta patagonica gen. et sp. nov.: a new ophthalmosaurid ichthyosaur from the Upper Jurassic of Patagonia and its palaeoecological implications

Lisandro Campos [1,2], Marta S. Fernández [1,2], Yanina Herrera [1,2] and Marianella Talevi [2,3]

[1]División Paleontología Vertebrados, Museo de La Plata, Facultad de Ciencias Naturales Y Museo, Universidad Nacional de La Plata. Av. 122 Y 60 La Plata, Argentina; [2]Consejo Nacional de Investigacione Científicas Y Técnicas (CONICET); [3]Universidad Nacional de Río Negro, Instituto de Investigación En paleobiología Y Geología, Río Negro, Argentina

ABSTRACT

Ophthalmosaurids were a globally distributed clade of ichthyosaurs that thrived from the Middle Jurassic to the early Late Cretaceous. Although their fossil record spans a wide palaeogeographic range, much of what is known about their anatomy and diversity derives from Late Jurassic localities in the Northern Hemisphere. In contrast, Late Jurassic forms from the Southern Hemisphere remain comparatively less known. Here we describe *Eternauta patagonica* gen. et sp. nov. a new ophthalmosaurid from the Tithonian deposits of the Vaca Muerta Formation. The holotype, previously referred to *Caypullisaurus bonapartei* Fernández, 1997, comprises a skull, teeth, a forelimb, and rib fragments. Phylogenetic analyses consistently recover *Eternauta* as a member of Platypterygiinae. Diagnostic features include a unique morphology of the pterygoid, an expanded postorbital contribution to the ventral margin of the orbit, and a retroarticular process that is strongly angled posterodorsally. These traits, together with a low jaw-opening mechanical advantage and relatively large sclerotic aperture, suggest a feeding strategy for capturing small, agile prey. The anatomical and functional features of *Eternauta* expand the known morphological and ecological disparity of Late Jurassic ophthalmosaurids, reinforcing the significance of the Vaca Muerta Formation as a key unit for understanding ichthyosaur evolution across the Jurassic – Cretaceous transition.

URN:lsid:zoobank.org:pub:68200526-150C-41 CD-8655-D250066BF215

ARTICLE HISTORY
Received 22 July 2025
Accepted 25 September 2025

KEYWORDS
Ichthyosaur; Jurassic; Patagonia; Vaca Muerta; Neuquén Basin

HANDLING EDITOR
Dr Rodrigo Temp Müller, Universidade Federal de Santa Maria, Brazil

Introduction

Ichthyosaurs were a diverse and ecologically successful clade of marine reptiles that thrived throughout most of the Mesozoic (McGowan & Motani, 2003). The earliest finds herald from the Early Triassic (Kear et al. 2023), and they rapidly acquired a suite of adaptations for life in open marine environments, and by the Jurassic all shared a thunniform body-plan associated with pelagic pursuit predation and sustained swimming (Massare, 1988; Motani, 2005). Since the Middle Jurassic, ophthalmosaurids had become the dominant ichthyosaur lineage, achieving a global distribution by the Late Jurassic – including high-latitude records – and maintaining high ecological diversity until their extinction in the early Late Cretaceous (Bardet, 1994; Delsett et al., 2017; Fischer et al., 2016; Roberts et al., 2014).

Although their fossil record spans a wide geographic range, much of what is currently known about ophthalmosaurid anatomy and diversity is based mainly on well-preserved specimens from Callovian to Tithonian localities in Europe (e.g. Bardet & Fernández, 2000; Jacobs & Martill, 2020; Moon & Kirton, 2016). In recent decades, however, discoveries from the Southern Hemisphere – particularly from various localities in Argentine Patagonia – have increased significantly, contributing to a more comprehensive and nuanced understanding of ichthyosaur evolution across the Jurassic – Cretaceous transition (e.g. Fernández et al., 2019). In this regard, the Tithonian – Berriasian marine deposits of the Vaca Muerta Formation (Neuquén Basin, Argentina) are particularly noteworthy. This unit hosts a diverse marine reptile assemblage – including thalattosuchians, thalassochelydian turtles, plesiosaurs, and notably, ophthalmosaurid ichthyosaurs – which provides key insights into marine ecosystems evolution during the end of the Jurassic (e.g. Gasparini et al., 2015; O'Gorman et al., 2018; Fernández et al., 2019; Herrera et al., 2021). Within the ichthyosaur material from the Tithonian levels of this unit, we re-examine

CONTACT Lisandro Campos lcampos@fcnym.unlp.edu.ar División Paleontología Vertebrados, Museo de La Plata, Facultad de Ciencias Naturales Y Museo, Universidad Nacional de La Plata. Av. 122 Y 60 La Plata, Argentina

Handling Editor Dr Mark T. Young School of GeoSciences, University of Edinburgh, United Kingdom of Great Britain and Northern Ireland.
Supplemental data for this article can be accessed online at https://doi.org/10.1080/08912963.2025.2568707

Published online 12 Oct 2025

MLP-PV 85-I-15–1, a specimen from Chacay Melehue locality (Neuquén Province, Argentina; Figure 1), previously referred to *Caypullisaurus bonapartei* Fernández, 1997 (Fernández, 1998). The new osteological observations and phylogenetic analysis support the recognition of this specimen as a new taxon, *Eternauta patagonica* gen. et sp. nov., which is distinguished by a unique combination of features in the postorbital region, palate and posterior mandible. The unusual orientation of the retroarticular process, along with other traits of documented palaeoecological importance, not only expands the known morphological disparity of Jurassic ophthalmosaurids but also provides new insight into their palaeoecology, reinforcing the status of the Vaca Muerta Formation as a key ichthyosaur-bearing unit for understanding Late Jurassic to Early Cretaceous evolutionary history of the lineage.

Institutional abbreviations

CAMSM, Sedgwick Museum of Earth Sciences, Cambridge, UK; **MACN**, Museo Argentino de Ciencias Naturales 'Bernardino Rivadavia', Ciudad Autónoma de Buenos Aires, Argentina; **MLP-PV**, Museo de La Plata, Paleontología Vertebrados, La Plata, Argentina; **MOZ-Pv**, Museo Provincial de Ciencias Naturales 'Dr. Prof. Juan A. Olsacher', Dirección Provincial de Minería, Zapala, Argentina.

Materials & methods

Phylogenetic analysis

To assess the internal phylogenetic relationships of Ophthalmosauridae, with special emphasis on *Eternauta patagonica* among ophthalmosaurids, we scored MLP-PV 85-I-15–1 in an expanded version of the dataset of Campos et al. (2024). This dataset was modified by incorporating two recently described ophthalmosaurid operational taxonomic units (OTUs): *Argovisaurus martafernandezi* Miedema et al., 2024 from the Bajocian (Middle Jurassic) and '*Platypterygius*' *elsuntuoso* Páramo-Fonseca et al., 2024 from the Barremian (Early Cretaceous). Additionally, we completed the character scoring for *Myobradypterygius hauthali* Huene, 1927 by integrating anatomical information from the specimens described by Pardo-Pérez et al. (2024). All modifications to the matrix were carried out using Mesquite v. 3.61 (Maddison & Maddison, 2019). The maximum parsimony analysis was conducted in TNT v. 1.5 (Goloboff & Catalano, 2016) using the implied weighting method, which mitigates the influence of homoplasy by assigning lower weights to characters in proportion to their level of homoplasy. We tested different values of the concavity constant ($k = 3$, $k = 5$, $k = 8$). This range was selected based on the matrix dimensions (131 characters and 55 OTUs) following the approach of Ezcurra (2024), who demonstrated a positive linear correlation between the optimal k-value range and the number of terminal taxa. Higher k-values progressively reduce the penalisation of homoplastic characters. For tree searches, we conducted a traditional heuristic analysis with 1000 replicates, using random addition sequences (RAS) and tree bisection and reconnection (TBR) branch-swapping algorithm, retaining up to 100 trees per replicate. To assess nodal support, we performed symmetric resampling with a 33% change probability, generating frequency difference values across 1000 replicates. The parsimony analysis was run for a second time using an equal weights approach and with a tree search under the exact same parameters detailed above. In this case, nodal support was calculated using Bremer support.

Palaeoecological inferences

To evaluate potential similarities and differences in the feeding ecology between the new taxon and other ichthyosaurs from the Neuquén Basin, we calculated the jaw opening mechanical advantage (OMA) following established methods (Ponstein et al., 2024; Westneat, 1994). This index quantifies the mechanical trade-off between force and velocity in mandibular depression, offering insights into feeding strategies and potential prey preferences. The mandibular lever system was analysed by measuring: (1) the input moment arm (distance from jaw joint to retroarticular process posterior edge) and (2) the output moment arm (distance from joint to anterior tip of the mandible), with OMA calculated as their ratio (Figure 2). The midpoint of the glenoid fossa represents the fulcrum. This index provides a biomechanical baseline for comparing jaw depression speed across taxa, where lower values indicate faster jaw opening and vice versa (Foffa et al., 2024; MacLaren et al., 2017). Measurements were taken from all known specimens recovered from Vaca Muerta Formation with a reasonably complete mandible: *Eternauta patagonica* (new taxon), *Caypullisaurus bonapartei* (MACN-N-32, MOZ-PV 6139), and an undescribed juvenile ophthalmosaurid (MLP-PV 83-XI -15–1). For comparisons, we included data from taxa with well-documented gut contents like *Stenopterygius quadriscissus* (Quenstedt, 1856) and '*Platypterygius*' *australis* (M'Coy, 1867) and those with feeding habits inferred from dental or cranial morphology, such as *Hauffiopteryx typicus* (von Huene, 1931), *Brachypterygius extremus* (Boulenger, 1904) and *Kyhytysuka sachicarum* (Cortés et al., 2021; Dick et al.,

2016; Foffa et al., 2018; Jamison-Todd et al., 2022; Kear et al., 2003; Páramo-Fonseca, 1997). This framework allows us to evaluate whether the OMA values of *Eternauta* align with those of the ichthyosaurs from the Vaca Muerta Formation or if the new taxon is a representative of a previously unnoticed functional diversity for this region of the paleopacific.

Palaeohistological analysis

Palaeohistological samples were taken from the dorsal rib of the MLP-PV 85-I-15–1. The transversal thin section was prepared using standard palaeohistological techniques and examined with light microscopy (Chinsamy & Raath, 1992). Nomenclature and definitions of structures used in this study are derived from Francillon-Vieillot et al. (1990) and Chinsamy-Turan (2005). Sections of this specimen were preliminarily reported for Talevi et al. (2012) and restudy here.

Systematic palaeontology

Ichthyosauria Blainville, 1835
Parvipelvia Motani et al., 1999
Ophthalmosauridae Baur, 1887

Eternauta gen. nov.

urn:lsid:zoobank.org:act:E06D57BE-2124–4958-B0B0-D9F65C6652AB

?*Platypterygius* Gasparini & Goñi, 1990, p. 303, pl. 2, Figure 4.

Diagnosis. As for the type and only species.

Eternauta patagonica sp. nov.

urn:lsid:zoobank.org:act:AB3E369E-11A3-4717-97E2-6E182C42C32A

Figures 3–9

Caypullisaurus bonapartei Fernández, 1998, p. 22, Figures 1–2.

Etymology. The genus name *Eternauta* combines the Latin *aeternus* ('eternal') and *nauta* ('sailor'), in reference to *El Eternauta* (1957) created by Héctor Oesterheld and Francisco Solano López, a seminal Argentine science fiction comic whose protagonist introduces himself as "*a navigator of time, a traveller of eternity, and a pilgrim of the centuries*". The specific epithet *patagonica* denotes the Patagonian region, where the holotype was discovered. Together, the name translates to '*The one who navigates eternally in Patagonia*' reflecting both its geographic origin and the enduring palaeontological legacy of marine reptiles in the region.

Holotype and only known specimen. MLP-PV 85-I-15–1, an almost complete skull mostly preserved on its right side, teeth, fragmentary rib and right forefin.

Occurrence. Chacay Melehue (37° 17'20'S; 70° 20' 45' W) Neuquén Province, Patagonia, Argentina. Mendoza Group, Vaca Muerta Formation (Tithonian), Upper Jurassic (Figure 1).

Diagnosis. Ophthalmosaurid ichthyosaur characterised by the following autapomorphies (marked with an *) and a unique combination of characters states: external naris completely divided into two lobes by means of a nasomaxillary pillar formed by contributions of the nasal and the maxilla (as in *Arthropterygius thalassonotus* Campos et al., 2020, *Baptanodon natans* (Marsh, 1879), *Parrassaurus yacahuitztli* Barrientos-Lara & Alvarado-Ortega, 2021a, *Simbirskiasaurus birjukovi* Ochev & Efimov, 1985, *K. sachicarum*, and most '*Platypterygius*' spp.); ventral portion of the postorbital constitutes more than half of the ventral margin of the orbit*; well-developed occipital lamella of the quadrate (as in *Ophthalmosaurus icenicus* Seeley, 1874, *Palvennia hoybergeti*; Druckenmiller et al., 2012, *Keilhauia*; Delsett et al., 2017, and *Leninia stellans* Fischeret al., 2014); triangular lateral lamella of the quadrate ramus of the pterygoid longer than the medial lamella; dorsal lamella of the pterygoid formed by a broad squared basis and terminates in an arrowhead-shaped tip*; retroarticular process of the mandible strongly posterodorsally angled*; tooth roots with round cross-section (shared with most non-Platypterygiinae ophthalmosaurids); humerus with three distal articular facets for the anterior accessory element (aae), radius and ulna (unlike '*Platypterygius*' spp., *B. extremus*, *Aegirosaurus leptospondylus* Bardet & Fernández, 2000, *Catutosaurus gasparinae* Fernández et al., 2021; *P. yacahuitztli*, *Sveltonectes insolitus* Fischer et al., 2011, and *Maiaspondylus lindoei* Maxwell & Caldwell, 2006); intermedium not contacting the humerus and supporting digits III and IV (as in *O. icenicus*, *Ca. gasparinae*).

Description

Taphonomy. Specimen MLP-PV 85-I-15–1 consists of a laterally compressed skull, mostly preserved in right lateral view (Figures 3 and 4). The postorbital region and most of the right mandibular ramus remain

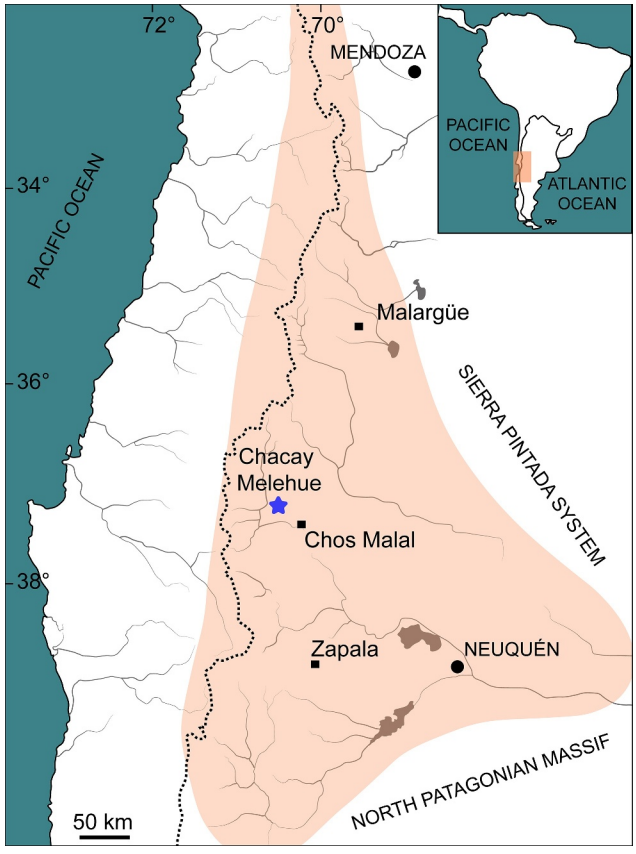

Figure 1. Map showing the geographic position of the Neuquén Basin and the Chacay Melehue locality (blue star) within Neuquén Province, Argentina.

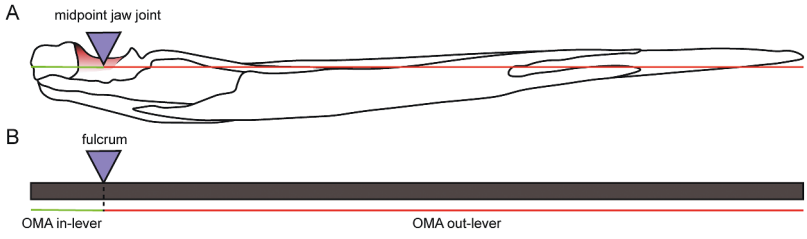

Figure 2. Schematic representation of opening mechanical advantage. A, illustration of an ophthalmosaurid lower jaw in medial view; B, lower jaw represented as a lever.

articulated. Compression has displaced the left premaxilla and nasal dorsally, such that they now lie above the right nasal. The right external naris is almost complete (Figure 5). The right quadrate has rotated along its longitudinal axis, revealing part of its anterior surface in lateral view whereas the left quadrate is completely disarticulated and exposed on the left side of the skull (Figures 6 and 7). Also, on the left surface of the skull, portions of the palatal complex are preserved in three dimensions, including both pterygoids and the left palatine (Figures 3(C,D), 7(A)). Most of the occipital region is missing, although the right supratemporal remains in place (Figure 6). Several premaxillary and dentary teeth are visible at the anterior end of the rostrum (Figure 8).

The right forelimb is incompletely preserved, three-dimensionally, and partially articulated (Figure 9). The humerus lacks part of the dorsal process. The zeugopodium is complete, although the ulna is displaced. Distal to the zeugopodium, the proximal carpals and part of the distal carpals are preserved.

Cranium—

Premaxilla. Both premaxillae are preserved, with the right one in anatomical position and the left one displaced (Figure 3). The right premaxilla is missing only a portion of the supranarial region. Several premaxillary

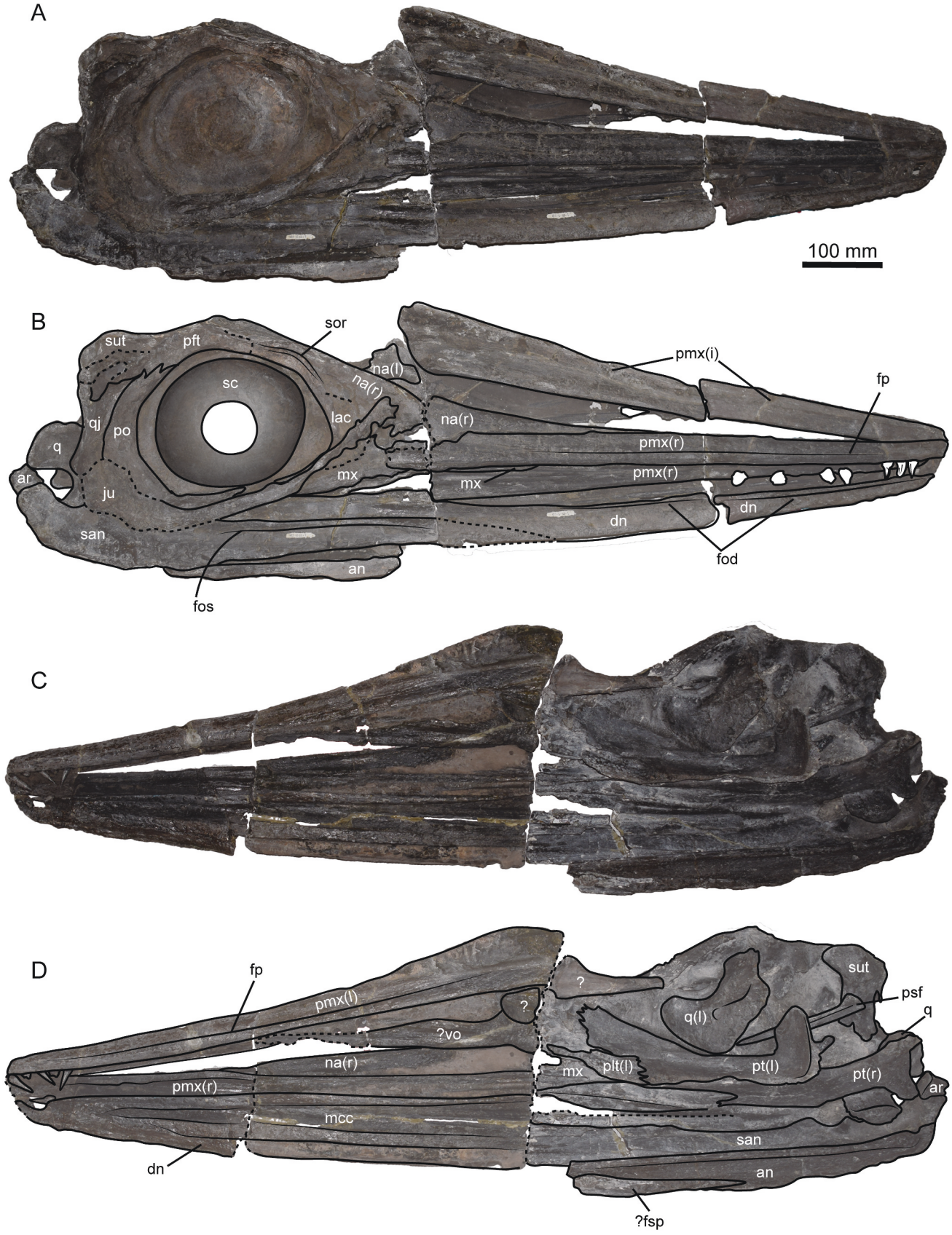

Figure 3. *Eternauta patagonica* gen. et sp. nov., holotype. MLP-PV 85-I-15–1, skull in A-B, right lateral view; C-D, ventral (palatal complex) and medial (mandible) views. an, angular; ar, articular; dn, dentary; fod, fossa dentalis; fos, fossa surangularis; fp, fossa praemaxillaris; fsp, splenial facet; ju, jugal; lac, lachrymal; mcc, symphysial portion of Meckelian canal; mx, maxilla; na, nasal; plt, palatine; pmx, premaxilla; po, postorbital; psf, parasphenoid; pt, pterygoid; q, quadrate; qj, quadratojugal; san, surangular; sc, sclerotic ring; sut, supratemporal; utf, upper temporal fenestra; vo, vomer.

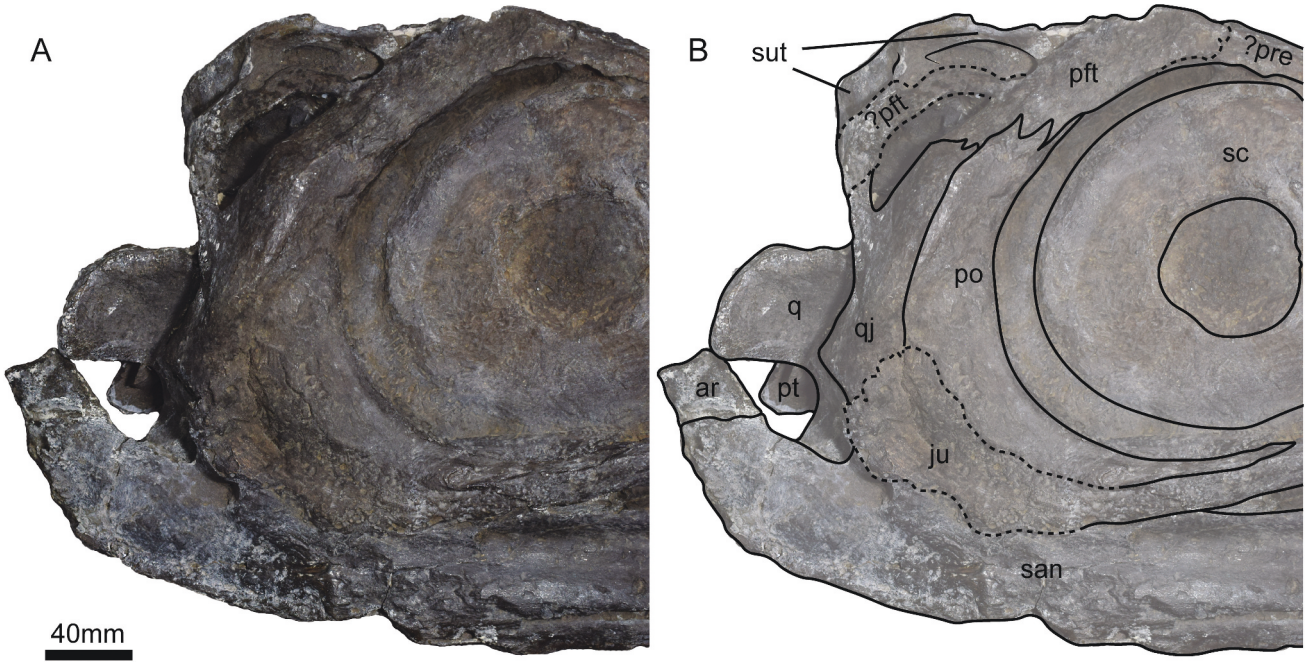

Figure 4. *Eternauta patagonica* gen. et sp. nov., holotype. MLP-PV 85-I-15–1, A, detail of the postorbital region of the skull in right lateral view; B, interpretation. ar, articular; ju, jugal; po, postorbital; pt, pterygoid; q, quadrate; qj, quadratojugal; san, surangular; sc, sclerotic ring; sut, supratemporal.

teeth are preserved, both within and outside the dental groove (Figures 3 and 7). The premaxillae are elongated and slender, with minimal height variation along the anteroposterior axis. In lateral view, the anterior end tapers to a point. On the lateral surface of the anterior portion of the premaxilla, the fossa praemaxillaris forms a shallow, continuous groove that extends posteriorly before fading out prior to the external naris (Figure 3 (A,B)). This fossa is located approximately 20 mm from the ventral margin of the premaxilla. Just below the external naris, the right premaxilla preserves part of the processus subnarialis, which extends beyond the anterior half of the external naris. However, its total extent is unknown as its posterior end is missing (Figure 5).

Maxilla. In lateral view, the maxilla contributes to the ventral and posterior margins of the external naris, with two low ascending processes (Figure 5). The anteriormost corresponds to the contribution of the maxilla to the nasomaxillary pillar which completely divides the external naris in two lobes. Ventrolateral to this process, the posterior portion of the processus subnarialis of the premaxilla overlaps the bone (Figure 5). The contribution of the maxilla to the posterior margin of the

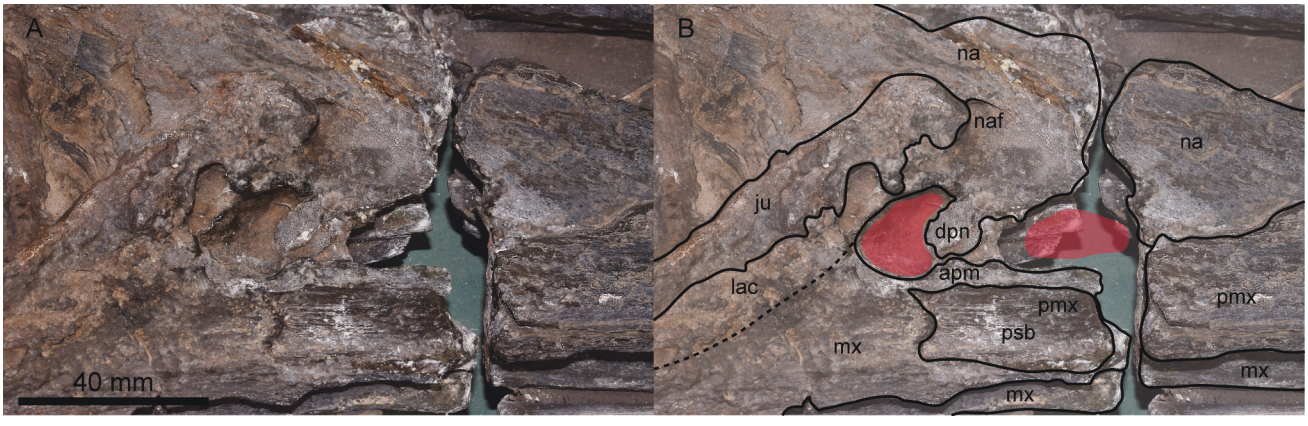

Figure 5. *Eternauta patagonica* gen. et sp. nov., holotype. MLP-PV 85-I-15–1, external naris in A, right lateral view; B, interpretation. apm; ascending process of the maxilla; dpn, descending process of the nasal; ju, jugal; lac, lachrymal; mx, maxilla; na, nasal; naf, nasal foramen; pmx, premaxilla; psb, processus subnarialis. Red shaded areas indicate the approximate location of the nasal lobes.

external naris constitutes the processus postnarialis. In this region, the damaged lachrymal prevents determining whether it was excluded from this margin or not by the maxilla. The anterior portion of the jugal is broken and displaced dorsally, exposing the jugal process. This structure extends only a short distance beneath the orbit (Figure 3(A,B)). Unfortunately, no maxillary teeth were preserved.

Nasal. The right nasal is preserved, with most of its length in anatomical position, except for its posterodorsal region (Figure 3(A,B)). It has an elongated triangular shape, with its anterior portion exceeding half the total length of the snout. In the narial region the nasals form part of the dorsal margin of the external naris and contribute to its division through a posteroventrally directed process that constitutes most of the nasomaxillary pillar (Figure 5). Posterodorsal to the external naris, on the lateral surface, the nasal bears a small oval-shaped foramen (Figure 5).

Lachrymal. Only the right lachrymal is preserved with its anterior region partially covered by the right jugal (Figures 3(A,B) and 5). The posterior edge of the lachrymal constitutes more than half of the anterior margin of the orbit. It also extends posteroventrally, forming the posterior process of the lachrymal, contributing to the ventral margin of the orbit alongside the jugal. This process ends before reaching the posterior half of the orbit (Figures 3(A,B)).

Prefrontal and postfrontal. Both elements are very fragmentarily preserved, preventing a detailed description. In the case of the prefrontal, the lateral surface bears marks indicating the position of the supraorbital crest, located above the anterodorsal portion of the orbit (Figure 3A,B).

Supratemporal. The main body of the right supratemporal is in anatomical position, with the rami largely preserved and the articular facets clearly visible; the facet for receiving the right parietal supratemporal process is not preserved, and a small portion of the anterior ramus is missing (Figures 3, 6 and Supplementary Figure S1). In lateral view, the ventral margin contacts the quadratojugal and postorbital (Figures 3(A,B) and Figures 4). The full anterior extent of this ramus is uncertain. In posterior view, the ventral ramus is short and medially contacts the occipital lamella of the quadrate and the dorsal lamella of the pterygoid, although the quadrate is displaced. Medial to this ramus, the stapedial process projects ventrally and is taller and more robust than the ventral ramus of the supratemporal (Figure 6). However, it is unclear whether the stapedial process reached the dorsal surface of the stapes, as most basicranial elements are collapsed or missing. At the junction between the stapedial process and the main body of the bone, a small depression marks the contact site between the supratemporal and the paraoccipital process of the opisthotic (Figure 6).

Postorbital. The postorbital exhibits the characteristic crescent shape and contributes to both the posterior and ventral margins of the orbit (Figure 3(A,B) and Figure 4). Its modest anteroposterior development at mid-orbital height results in a relatively narrow contribution to the postorbital region. Dorsally, it articulates with the supratemporal and postfrontal, although the relationships between these elements are difficult to discern, as most sutures in this region leave only subtle marks. Posteriorly, the postorbital articulates via a vertical, simple, and straight suture with the quadratojugal. The ventral portion of the postorbital is unique among Ophthalmosauridae due to its anterior extension, which surpasses half the anteroposterior length of the orbit (Figure 3(A,B), 4).

Quadratojugal. The quadratojugal articulates anteriorly with the postorbital, medially with the quadrate, and dorsally with the supratemporal. As is the case for the postorbital its lateral exposure is small, and its anteroposterior extent is short. Ventrally, the lateral surface of the quadratojugal is almost entirely covered by the ascending process of the jugal. The lateral surface is completely smooth, similar to that of the postorbital (Figures 3(A,B), 4), making it unlikely that the squamosal was present in the postorbital region of this specimen. For this reason, the absence of this element is interpreted as a genuine feature rather than a preservation artefact.

Jugal. This element is in near-anatomical position along most of its length but is disarticulated and dorsally displaced at its anterior end, overlapping parts of the lachrymal, the right nasal, and the external naris (Figures 3(A,B), 4 and 5). The jugal has a 'J' shape, with a horizontal bar extending anteroposteriorly beneath the orbit and an ascending process in the postorbital region. The horizontal bar is low and straight throughout its length, with a flat lateral surface. The anterior region of the suborbital portion of the bar articulates ventrally with the posterior process of the lachrymal. Most of the ascending process is preserved as an impression on the postorbital and the quadratojugal. This process is broad, with a rounded and concave

dorsal margin that contacts the postorbital and the quadratojugal (Figures 3(A,B) and 4).

Pterygoid. Both pterygoids are almost completely preserved, with only the anterior margins (the region immediately anterior to the interpterygoid vacuities) inaccessible for description. The right pterygoid retains the contact with the pterygoid lamella of the right quadrate (Figure 6 and Supplementary Figure S2). The left pterygoid is disarticulated and lies above the right one, with its anterior end still articulating with the left palatine (Figures 3(C,D)). In ventral view, the bone is divided into two regions: an anterior or palatal ramus and a posterior or quadrate ramus, separated by a mediolateral constriction (Figure 7A). The palatal ramus is further subdivided anteriorly into two regions: a medial region, which is more elongated anteroposteriorly, and a shorter lateral region. Both regions progressively narrow towards their anterior ends. The medial region forms a long anterior process that curves medially, defining the anterior and lateral margins of the interpterygoid vacuity. The medial edge of this region increases in height and thickness posteriorly, from the anterior tip of the process to the constriction separating the two rami. The lateral region of the palatal ramus originates from a lateral expansion beginning anterior to the constriction between the palatal and quadrate rami. Its anterior end articulates with the palatines through an interdigitated suture and forms the postpalatinus process. Posterior to this suture, the ventral surface of the pterygoid is subtly concave, marking the insertion site for the Musculus adductor mandibulae internus pterygoideus (Figure 7A). In posterior view, the quadrate ramus is triradiate due to the development of three lamellae oriented dorsally, lateroventrally, and medially (Figure 6, Supplementary Figure S2). In lateral or medial view, the dorsal lamella appears rectangular, with a broad base that narrows dorsally into a triangular end separated by a subtle ridge (Figure 3(C,D)). This lamella is the longest of the three. The lateral lamella is

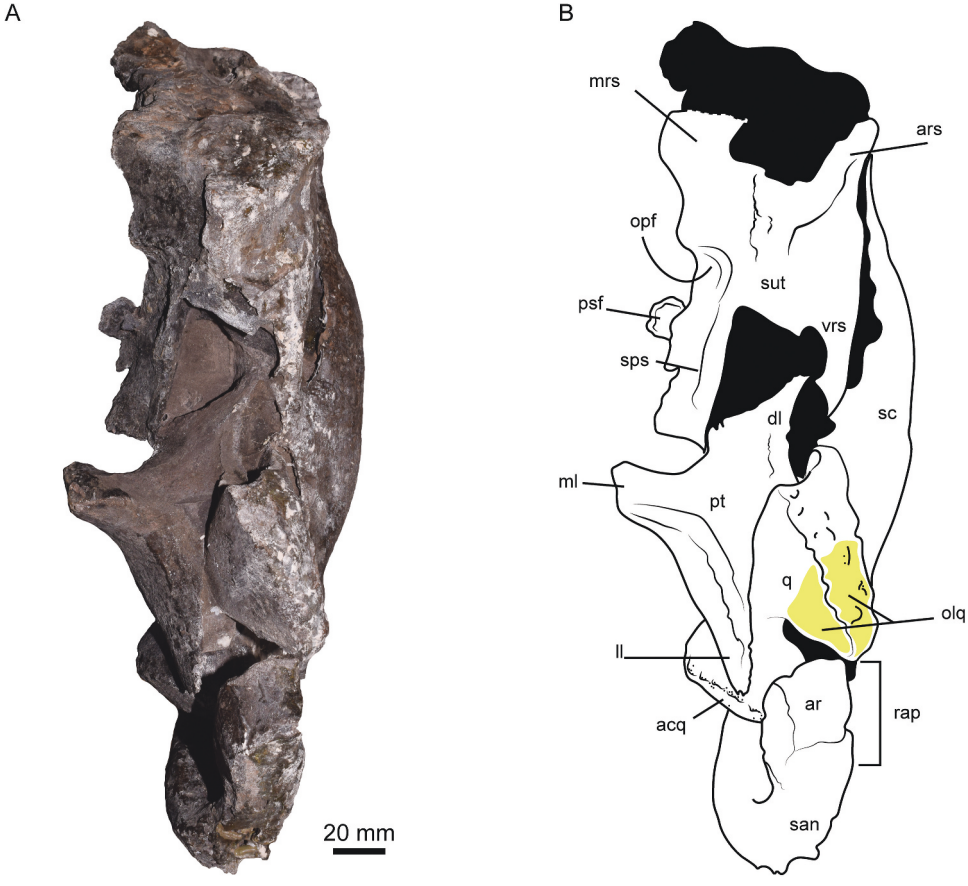

Figure 6. *Eternauta patagonica* gen. et sp. nov., holotype. MLP-PV 85-I-15–1, skull in A, posterior view; B, interpretation. acq, articular condyle of the quadrate; ar, articular; ars, anterior ramus of the supratemporal; dl, dorsal lamella of the pterygoid; ll, lateral lamella of the pterygoid; ml, medial lamella of the pterygoid; mrs, medial ramus of the supratemporal; olq, occipital lamella of the quadrate; opf, opisthotic facet; pt, pterygoid; psf, parasphenoid; q, quadrate; rap, retroarticular process; san, surangular; sc, sclerotic ring; sps, stapedial process; sut, supratemporal; vrs, ventral ramus of the supratemporal. Yellow coloured areas indicate the posterior and dorsal surfaces of the occipital lamella.

Figure 7. *Eternauta patagonica* gen. et sp. nov., holotype. MLP-PV 85-I-15–1, A, right pterygoid in ventral view; B, left quadrate in medial view. acq, articular condyle of the quadrate; foq, quadrate foramen; fst, stapedial facet; ll, lateral lamella of the pterygoid; mame, Musculus adductor mandibulae externus attachment point; mamip, Musculus adductor mandibulae internus pterygoideus attachment; ml, medial lamella of the pterygoid; stg, supratemporal groove. Black arrows highlight the constriction delimiting the separation between the palatal and quadrate rami of the pterygoid.

triangular in posterior view, with a broad base but lacking a ridge separating it from the tip. The surface formed by the dorsal and lateral lamellae is markedly concave, accommodating the medial surface of the quadrate. The medioventral lamella is the least developed of the three in posterior view (Figure 6, Supplementary Figure SXX). The dorsal surface of the pterygoid is irregular and rugose, indicating the presence of cartilage in life. This region facilitated contact between the pterygoid, the ventral surface of the basisphenoid, and the basipterygoid processes.

Quadrate. The right quadrate is completely preserved, although slightly rotated on its axis, exposing part of its anterior surface in right lateral view (Figures 3(A,B) and 7 (A)). The left quadrate is disarticulated, with its medial surface fully exposed (Figures 3(C,D) and 7B). In both lateral and medial views, the quadrate has a 'C' shape, with a well-developed occipital lamella dorsally and a pterygoid lamella positioned anteriorly and ventrally to it, with the articular condyle at its ventral end. When the quadrate is placed in anatomical position, the occipital lamella is oriented posterolaterally, while the pterygoid lamella faces medially. Between these structures lies a large lateral concavity, representing the quadrate foramen (Figure 7(B)), whose lateral margin is formed by the quadratojugal. Much of the medial surface of the right quadrate is covered by the quadrate ramus of the right pterygoid, leaving only its dorsal portion and the articular condyle exposed (Figure 6 and Supplementary Figure S3). Conversely, the medial surface of the left quadrate is entirely exposed, revealing a shallow vertical groove extending from the dorsal region to the stapedial facet, marking the contact between the quadrate and the supratemporal. The stapedial facet is circular and formed by a depression located at the mid-height of the medial surface (Figure 7(B)). The articular condyle is a massive and robust structure, with an irregular and rugose surface indicating cartilage coverage in life (Figure 7(A)). Due to displacement during compression, the condyle is positioned above the process for the Musculus adductor mandibulae externus on the surangular. Immediately anterior to the condyle, the ventral margin of the

quadrate becomes concave, marking the quadrate neck (Figure 7(B)).

Parasphenoid. A fragmentary portion of the parasphenoid is preserved lying next to the stapedial process of the supratemporal (Figures 3(C,D)). It is straight all along its length and triangular in cross-section.

Palatine. The left palatine is still in its anatomical position, articulating through an interdigitating suture with the pterygoid and with its dorsal surface exposed (Figures 3(C,D)). It comprises a roughly rectangular and thin posterior plate that contacts posterolaterally the pterygoid and an elongated anterolateral process for the reception of the maxilla. The anterior margin of the posterior plate curves posteriorly, defining the posterior border of the internal narial opening.

Mandible—

Dentary. The right dentary is fractured in three parts but still in anatomical position (Figure 3). In lateral view, at the anterior end of the dentary, there is a continuous and shallow groove running anteroposteriorly. This groove is located closer to the dorsal margin of the dentary than to the ventral margin and is recognisable along the anterior two-thirds of the lateral surface. In medial view, the surface is severely damaged, although the groove corresponding to the Meckelian canal can still be roughly traced, as the right splenial is not preserved (Figures 3(C,D)). This canal runs anteroposteriorly along the medial surface of the dentary, being lower at the anterior end and becoming higher posteriorly. In dorsal view, the dentary shows a deep and continuous alveolar groove, in which no distinguishable alveoli are formed (Figure 8). Only a single tooth has been preserved within the groove, although displaced from its anatomical position, as it is preserved horizontally with the apical end of the crown pointing anteriorly.

Surangular. The right surangular is almost complete, with only the most anterior ventral portion missing. It is in its anatomical position, articulating ventrally with the angular and posterodorsally with the articular (Figures 3–4 and Supplementary Figure S3). In lateral view, the surangular is straight anteroposteriorly along most of its length, except for the posterior portion, which is strongly curved posterodorsally. This posterior curvature contributes to forming a deep glenoid fossa, although its exact extent cannot be determined due to slight displacement of the articular. Just anterior to this fossa, on the medial surface of the surangular, is the robust conical process for the insertion of the Musculus adductor mandibulae externus, oriented dorsomedially (Figure 7(A)). On the lateral surface, around the midpoint of the orbit, a shallow, continuous groove (fossa surangularis) originates and extends anteriorly, disappearing before the anterior end of the surangular contacts the dentary (Figures 3(A,B)).

Angular. Only the medial portion of the right angular and a fragment of the lateral surface have been preserved, exposed ventrolaterally to the surangular (Figure 3). In medial view, the angular is slightly separated from the medial surface of the surangular, creating a groove along which the prearticular would have articulated in life (Figure 3, Supplementary Figure S3). Anteriorly, the angular extends beyond the paracoronoid process of the surangular; however, its full extent cannot be determined with certainty, as much of the anterior region of the angular would have been covered by the splenial in life. Although the splenials have not been preserved and the ventral margin of the angular is damaged, the facet for the splenial can still be observed on the preserved ventral margin of the angular. This facet is elongate and triangular in shape, terminating posteriorly in a sharp point (Figures 3(C,D)).

Articular. The right articular is preserved but slightly displaced from its anatomical position, such that its posterior surface now faces posterodorsaly, and a small portion of its lateral surface – normally concealed by the surangular – is exposed laterally (Figures 3–5). In medial view, the element is anteroposteriorly longer than dorsoventrally high rectangular, with a subtly convex anterior margin (Suplementary Figure S3).

Dentition—

A total of 21 teeth have been preserved, of which 14 are still associated with the premaxillae, one with the left dentary, and the remaining six are disassociated. None of these elements are complete, and in several cases, they are represented only by a fragment of the root still attached to the alveolar grooves, or by the isolated fragmentary crowns (Figure 8). The crown is characterised by being conical, slender, and with no signs of curvature in any direction. Its surface is covered by a thin layer of enamel, which defines a series of shallow grooves and delicate striations running in the apicobasal direction. The height of the crowns ranges between 15 and 20 mm. The basal margin of this enamel layer is diffuse, with no distinct transition between it and the acellular cementum ring. The acellular cementum ring has a smooth surface and lacks any ornamentation or other structures. The root surface is covered by a series of fine, delicate striations running parallel in the

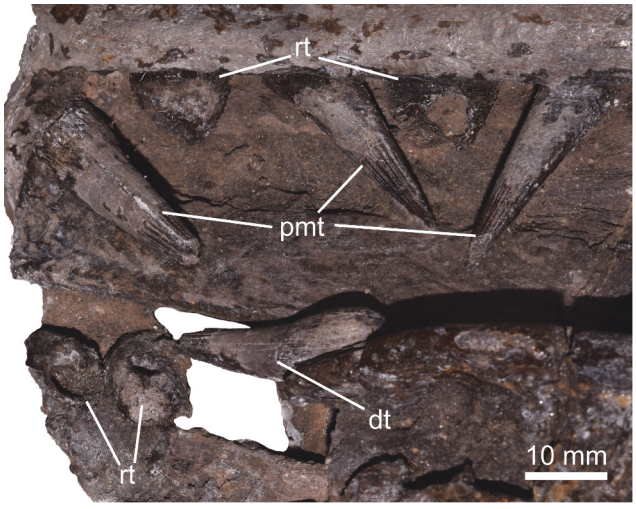

Figure 8. *Eternauta patagonica*, holotype. MLP- PV 85-I-15–1, rostrum and teeth. dt, dentary tooth; pmt, premaxillary teeth; rt, roots.

apicobasal direction; however, the spacing between these striations is much narrower compared to those on the crown. In cross-section, the root is circular in shape.

Forefin—

General aspects

Only part of the right limb is preserved, partially articulated with the zeugopodium and distal elements beyond it. Additionally, associated with the right limb is an elongated, recurved element, which is interpreted as a rib fragment (Figure 9).

Humerus. The right humerus is preserved in three dimensions, with no signs of plastic deformation, and is missing only the proximal region of the dorsal surface, including part of the dorsal process. Both the proximal and distal ends exhibit similar anteroposterior development, with the latter being slightly wider. The proximal epiphysis is approximately rectangular, with a rough surface indicative of a cartilaginous covering in life. In dorsal view, the humeral surface shows some damage to its proximal portion. However, the anterodistal region of the dorsal process is still preserved. The process is plate-like and arises from the posteroproximal margin of the dorsal surface and extends diagonally in anterodistal direction (Figure 9A). Similar to the deltopectoral crest, it is robust, with its distal end reaching halfway along the humerus. The deltopectoral crest is triangular, originating at the proximal end of the anterior half of the ventral surface and extending distally beyond the proximal half of the bone (Figure 9B–D). In anterior view, the proximal epiphysis is markedly widened due to the development of the dorsal process and the deltopectoral crest. From this view it can be seen that the ulnar facet of the humerus is significantly displaced ventrally (Figure 9C). Distally, the humerus presents three articular facets: one anterior for the accessory anterior element, one medial for the radius, and one posterior for the ulna. Radial and ulnar facets present similar lengths in ventral/dorsal view. The only facet whose surface can be observed is the ulnar one, due to the disarticulation of the ulna. This facet is rounded in shape, with a rough and strongly concave surface (Supplementary Figure S4). Additionally, this facet is not only displaced ventrally relative to the radial and accessory anterior facets but is also inclined proximally, forming an acute angle of approximately 40° with the radial facet, which faces distally (Figure 9B).

Zeugopodium. The anterior accessory element and radius are articulated, whereas the ulna and the row of distal elements are moderately displaced from their anatomical position (Figures 9(A–C)). For this reason, the ulna is only visible in dorsal view, while the ulnar facet is only visible in ventral view (Figures 9(A,B)). The aae is located anterior to the radius and has a droplet shape, resulting in a very narrow proximal articular facet for the humerus and a broader, convex distal end (Figures 9(A,B)). Anteriorly, this element is strongly compressed, defining a very thin anterior margin (Figure 9C). The radius is pentagonal, wider than long, and mostly visible in ventral view (Figures 8(A,B)). The articular facet for the humerus is horizontal and straight although its edge is damaged. The articular facet for the accessory anterior element is also straight, oriented proximodistally. The distal margin is incomplete, although in dorsal view, it is possible to discern the articulation of the radius with the radiale (Figure 8A). The posterior margin of the radius is convex, defining the articular facet for the ulna (Figure 9B). The ulna is rectangular, with slightly convex and rounded margins (Figure 9B). Anteroposteriorly, it is shorter than the radius (Figure 9B).

Carpals. The proximal carpals are preserved but displaced from their anatomical positions. The radiale and ulnare closely resemble the radius and ulna, respectively. The radiale is also pentagonal in shape, although its posterior margin is less convex than that of the radius (Figure 9A). The intermedium is incomplete, with only its distal portion preserved; two articular facets, obliquely oriented to one another, can be distinguished (Figure 9B). These facets can be confidently identified

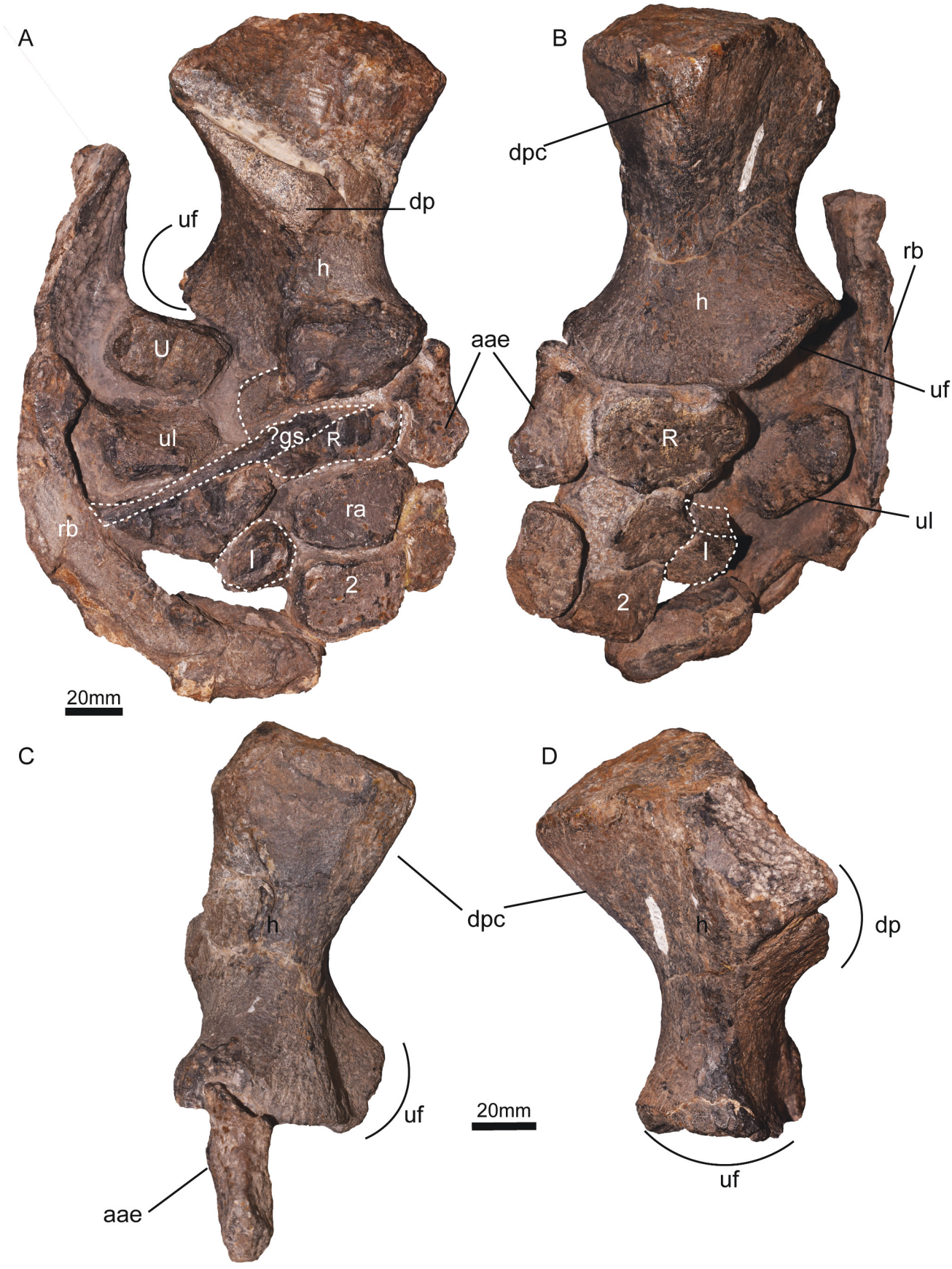

Figure 9. *Eternauta patagonica*, holotype. MLP- PV 85-I-15–1, right forefin in A, dorsal; B, ventral; C, anterior and D, posterior views. aae, anterior accessory element; dp, dorsal process; dpc, deltopectoral crest; gs, gastralia; h, humerus; I, intermedium; R, radius; ra, radiale; rb, rib; U, ulna; ul, ulnare; uf, ulnar facet; 2, distal carpal 2.

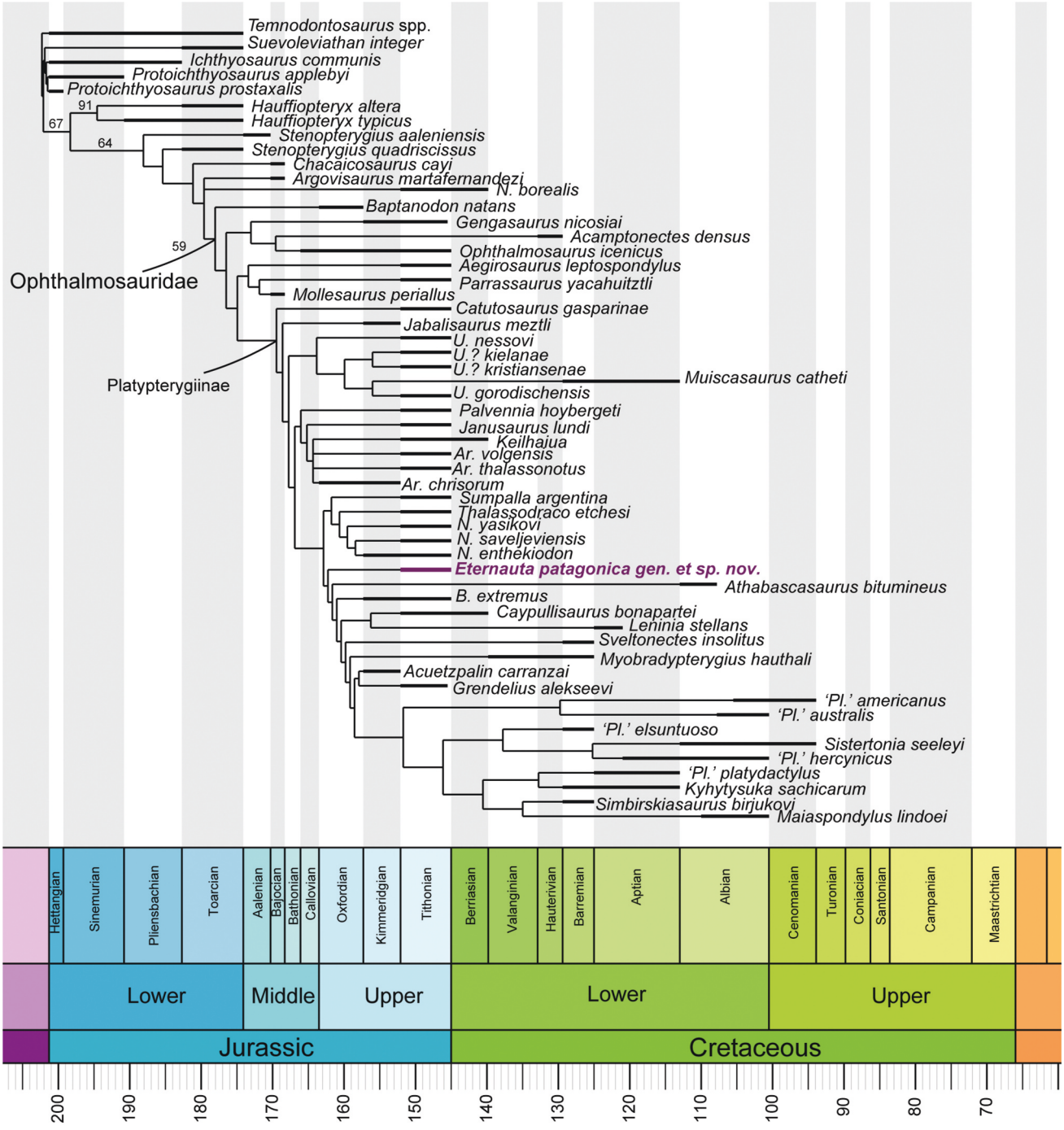

Figure 10. Time-calibrated strict consensus arising from implied weighting ($k = 3$) maximum parsimony analysis, in 'equal' reconstruction branches lengths. Branch values of resampling ≥50 are indicated over the branches.

as those for distal carpals 3 and 4, as distal carpal 2 remains in articulation with the radiale.

Phylogenetic analyses

Phylogenetic analyses conducted using maximum parsimony with implied weighting produced three most-parsimonious trees (MPTs) under a concavity constant of $k = 3$, with a tree length of 59.75921 (Figure 10). These trees exhibit a consistency index (CI) of 0.240 and a retention index (RI) of 0.540. When the concavity constant was increased to $k = 5$, the analysis resulted in three MPTs with a length of 47.12532, along with marginally higher consistency and retention indices (CI = 0.246; RI = 0.556) (Supplementary Figure S5). Further increasing the concavity constant to $k = 8$ yielded two MPTs with a length of 35.8395, though with slightly lower indices (CI = 0.206; RI = 0.442) (Supplementary

Figure S6). Regardless of whether penalties are applied to homoplastic characters or if equal weights are employed, Ophthalmosauridae is recovered as a well-supported clade (Figures 10–11). The implementation of the strongest penalisation ($k = 3$), retrieves three synapomorphies for Ophthalmosauridae: presence of plate-like dorsal ridge on the humerus (ch. 102–1), loss of notching on the elements of the leading edge of the forefin (ch. 113–1) and the presence of at least one anterior accessory digit (ch. 117–1). *Eternauta patagonica* is retrieved as a basal member of a clade of platypterygiines formed mostly by Cretaceous taxa and Late Jurassic forms like *Brachypterygius extremus*, *Caypullisaurus bonapartei*, *Grendelius. alekseevi* and *Ac. carranzai* Barrientos-Lara & Alvarado-Ortega, 2020. This node is diagnosed by the presence of a lateral lamella of the pterygoid more mediolaterally developed than the medial lamella (ch. 8–0). When lower penalisations are applied ($k = 5$, 8) Ophthalmosauridae is diagnosed on the basis of four synapomorphies: basipterygoid processes markedly expanded laterally (ch. 46–1), extracondylar area of the basioccipital moderately developed in such a way that its expansion in any direction (lateral and/or ventral) is less than half the height of the occipital condyle (ch. 50–1), an extensive lateral exposure of the angular, exceeding that of the surangular (ch. 78–1) and a complete fusion of the atlas-axis without visible suture (ch. 83–1). *Eternauta patagonica* is recovered as the sister taxa of a small clade containing *Sumpalla argentina* Campos et al., 2021, *Gengasaurus nicosiai* Paparella et al., 2017, and *Acamptonectes densus* Fischer et al., 2012. This node is diagnosed based on the morphology of the nasals and the external naris (ch. 12–1, ch. 13–1, ch. 14–1).

In the case of the analysis using equal weights it resulted in 44 MPTs of 618 steps (CI = 0.249; RI = 0.562). Ophthalmosauridae is diagnosed based on the loss of sagittal eminence on the parietals (ch. 28–1), and the same traits as in the analyses using concavity constants of 5 and 8. The strict consensus partially resolves the ophthalmosaurid ingroup, recovering *A. martaferandezi* as the basal-most member of the group. Internally, the resolution of the rest of the ophthalmosaurids is moderate, with several Jurassic and Cretaceous taxa falling into a polytomy or as part of small clades. The IterPCR protocol (Pol & Scapa, 2009) identified *L. stellans* and *Athabascasaurus bitumineus* Druckenmiller & Maxwell, 2010 as unstable taxa, both exhibiting more than 50% missing data for the cranium and mandible and over 75% missing data for the postcranium (Supplementary Figures S7,S8). Ignoring the alternative positions of the aforementioned taxa increases the resolution of the consensus retrieving nine additional nodes (Figure 11). As in the searches using implied weighting, *E. patagonica* is found as sister taxa of a clade containing *Su. argentina*, *Ge. nicosiai* and *Ac. densus* and sharing nasals and external naris characteristics.

Histology and microstructure

At the macroscopic level, the transverse section of the rib displays a circular outline and relatively small size (Supplementary Figure S9A). The structure is characterised by a large medullary cavity occupying a substantial proportion of the cross-sectional area (Supplementary Figure S9B). Within this cavity, isolated fragments of broken trabeculae are evident. The absence of any signs of fracturing or pathology suggests that the presence of these trabeculae is attributable to diagenetic processes.

In the perimedullary region, trabeculae are lined with lamellar bone tissue. Cement lines are discernible within these structures, demarcating the successive lamellae (Supplementary Figure S9C). Osteocyte lacunae are fusiform to elliptical in shape, with their long axes aligned with the orientation of the surrounding lamellae. Although numerous, these lacunae are not densely packed.

Towards the cortical region, several resorption spaces are present, all bordered by lamellar tissue. Although the outermost compact cortical layer is not preserved in the section, its reduced thickness can be inferred. The sampled tissue is predominantly secondary in nature, as evidenced by the abundance of secondary osteons distributed across the section.

The histological features of the bone tissue preclude the possibility that the specimen belonged to an osteologically immature individual. On the contrary, the presence of extensively remodelled secondary trabecular bone, the abundance of resorption spaces bordered by lamellar tissue, and the absence of primary bone, cartilage, or other indicators of early ontogenetic stages support the interpretation that the individual was osteologically mature. This conclusion is consistent with observations reported by Talevi et al. (2012) for ribs and by Talevi et al. (2021) for phalanges of other ichthyosaur specimens.

Discussion

Comparison of *Eternauta* with *Caypullisaurus*

The holotype of *Eternauta patagonica* gen. et sp. nov. (MLP-PV 85-I-15–1) was first mentioned and tentatively assigned to the genus '*Platypterygius*' by

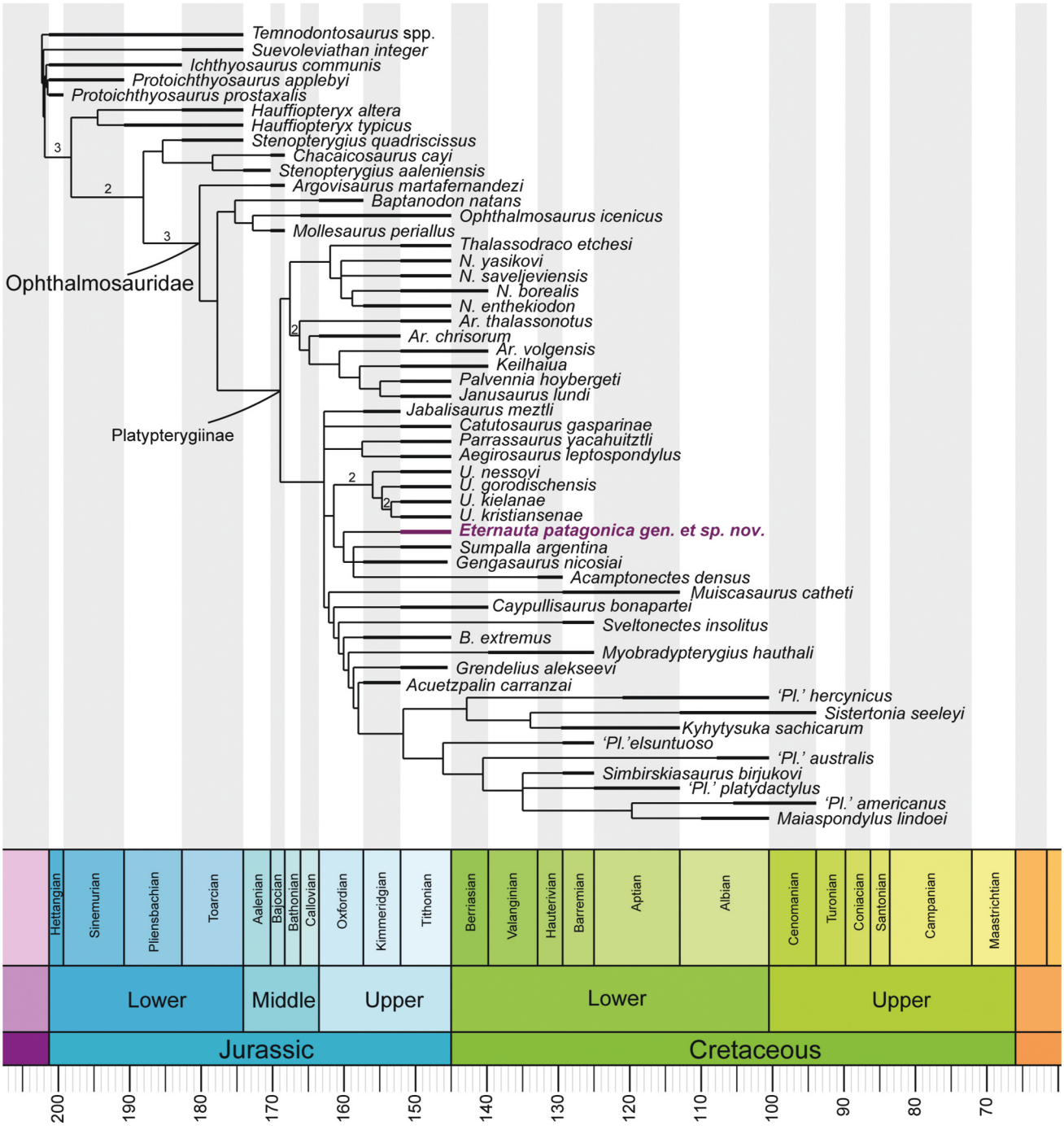

Figure 11. Time-calibrated strict consensus arising from unweighted maximum parsimony analysis, in 'equal' reconstruction branches lengths. Nodal support > 1 is indicated.

Gasparini and Goñi (1990), although these authors did not provide an osteological description of the specimen or a justification for this assignment. A decade later, Fernández (1997) described two ophthalmosaurid specimens and established the genus and species *Caypullisaurus bonapartei*. The following year, Fernández (1998) redescribed the specimen MLP-PV 85-I-15–1 and concluded that it belonged to *Cay. bonapartei*. This reassignment was based on shared features of the rostrum, the shape of the external naris, and the forelimb (Fernández, 1998). However, the re-examination of MLP-PV 85-I-15–1 here conducted has revealed several differences from *Cay. bonapartei*.

The external naris of *Cay. bonapartei* is characterised by being elongated and simple, lacking structures

indicative of any division (Fernández, 1997, 2007), except possibly in the specimen MOZ-PV 6139 (L. Campos pers. obs. 2023). However, the morphology of the external naris in MLP-PV 85-I-15–1 differs substantially from that of *Cay. bonapartei*. In *Eternauta*, the maxilla bears a robust ascending process, which, despite being fragmentary, can be observed protruding into the external naris from the ventral margin (Figure 5). Similarly, the nasal presents a descending process that extends from the dorsal region of the external naris (Figure 5). Additionally, the lateral exposure of the anterior process of the maxilla is short in *Eternauta*, whereas in *Cay. bonapartei*, it is considerably longer.

The most notable cranial differences are found in the postorbital region. *Caypullisaurus bonapartei* is characterised by a well-developed anteroposteriorly elongated postorbital region, with a broad lateral exposure of the quadratojugal and a well-developed ventral margin, a robust postorbital restricted to the posterodorsal margin of the orbit, and a rectangular squamosal (Fernández, 1997, 2007). In contrast, *Eternauta* exhibits markedly different features: the postorbital region is only weakly developed anteroposteriorly, the quadratojugal is poorly exposed laterally, and its ventral margin is poorly developed. The postorbital contributes significantly to the ventral margin of the orbit, extending beyond half of its anteroposterior length, and there is no indication of a squamosal, as seen in other platypterygiinae ophthalmosaurids (e.g. Kear, 2005). The mandible also differs substantially from that of *Cay. bonapartei*, particularly in the morphology of the posterior region. In the latter, the retroarticular process is robust and oriented almost horizontally in lateral view, whereas in *Eternauta*, this region is gracile and strongly inclined dorsally (Figure 3A,B, Supplementary Figure S3).

Although the preserved forefin elements of MLP-PV 85-I-15–1 are scarcer than those known for *Cay. bonapartei*, differences can still be identified at the zeugopodial level. In *Cay. bonapartei*, the aae is quadrangular, establishing broad contact with the humerus (Fernández, 2001), whereas in *Eternauta*, this element is teardrop-shaped and forms a narrow contact with the humerus (Figure 9A–C).

Finally, it is worth noting that the intermedium of *Eternauta* has two distal facets indicating that articulated with two distal carpals, supporting two digits (Figure 9). In *Cay. bonapartei*, by contrast, the intermedium supports only digit 3 (Fernández, 1997, 2001).

Comparison of *Eternauta* with other ophthalmosaurids

Middle Jurassic to Late Cretaceous ichthyosaurs can be readily distinguished from *Eternauta* based on the morphology of the postorbital region of the skull, pterygoids, mandible and the forefin.

The postorbital region of the skull in *Eternauta* is slender, with subequal lateral exposition of the postorbital and the quadratojugal and lack of squamosal bone. In the only known Bajocian ophthalmosaurid taxa, *Mollesaurus periallus* Fernández, 1999 and the recently described *Argovisaurus martafernandezi*, both lack preserved forefins, so comparisons are limited to cranial and dental features. In *M. periallus*, the postorbital region is broad, with a quadratojugal that exhibits narrow lateral exposure and a well-developed squamosal bone (Fernández & Talevi, 2014). Its teeth display a distinct pattern of ornamentation, with striations predominantly on the labial surface of the crown, while the lingual side remains nearly smooth (Fernández & Talevi, 2014). In contrast, *Eternauta* exhibits longitudinal striations encircling the entire crown.

The postorbital region of *A. martafernandezi* and its dentition are too incomplete for detailed comparisons, although it is worth noting that the squamosal was present in this taxon (Miedema et al., 2024). In some ophthalmosaurine-grade ophthalmosaurids, such as *Ba. natans* and *O. icenicus*, the postorbital region is slender and characterised by the presence of a triangular squamosal bone (Gilmore, 1906; Moon & Kirton, 2016). This feature is also present in some Tithonian ophthalmosaurids, including *Aegirosaurus leptospondylus* and *Thalassodraco etchesi* Jacobs & Martill, 2020, although in the latter, the postorbital is notably robust (Bardet & Fernández, 2000; Jacobs & Martill 2020). Among recently described ophthalmosaurids from the Late Jurassic of Mexico, *Jabalisaurus metzli* Barrientos-Lara & Alvarado-Ortega, 2021b also presents a triangular squamosal bone (Barrientos-Lara & Alvarado-Ortega, 2021b). Another common character present in the aforementioned taxa is a quadratojugal almost entirely covered laterally by the postorbital. In all specimens referred to *Nannopterygius* von Huene, 1922, where the postorbital region is partially preserved, including the holotype of the type species *Nannopterygius enthekiodon* (Hulke, 1871), preservation prevents the assessment of the relationship between the postorbital and the quadratojugal (Moon & Kirton, 2018; Zverkov & Jacobs, 2021). However, in this genus, the presence of a well-developed triangular squamosal is unambiguous (Moon & Kirton, 2018; Zverkov & Jacobs, 2021). Likewise, *Undorosaurus*? *kristiansenae*, from the Tithonian of Svalbard, also exhibits a triangular squamosal (Zverkov & Efimov, 2019). Conversely, *Eternauta* lacks a squamosal bone, a condition also found in some

Cretaceous taxa such as '*Platypterygius*' spp (e.g. Kear, 2005; Páramo-Fonseca et al., 2024). While this difference could potentially be attributed to a taphonomic artefact – given that other elements of the postorbital region, such as the ascending process of the jugal, were also lost – contact marks left by these elements on adjacent bones confirm their original presence. In contrast, there is no evidence of a squamosal at the contact between the quadratojugal and the supratemporal, suggesting that its absence is not merely a result of preservation bias.

The pterygoids of *Eternauta* exhibit a distinctive combination of traits, including a *processus postpalatinus*, a triangular lateral lamella that is more mediolaterally developed than the medial lamella, and a dorsal lamella with a remarkably broad base and a triangular tip, giving it an arrowhead-like shape in posterior view. Together, these features make this element unique among ichthyosaurs. The *processus postpalatinus* is present in many non-ophthalmosaurid parvipelvians, such as *Hauffiopteryx typicus* and *Stenopterygius quadriscissus* (Maxwell & Cortés, 2020; Miedema & Maxwell, 2022). Among ophthalmosaurids, this structure is not widely represented and has only been reported in *Baptanodon natans* and *Catutosaurus gaspariniae*, both from the Late Jurassic (Fernández et al., 2021; Gilmore, 1906). In all Cretaceous ophthalmosaurids for which the pterygoid is known, this process is absent (e.g. Kear, 2005). The presence of a lateral lamella that is more mediolaterally developed than the medial lamella in the quadrate ramus of the pterygoid is shared with *M. periallus* (Fernández & Talevi, 2014: Figure 2k). Similarly, a dorsal lamella with a broad, quadrangular base has been reported in at least two ophthalmosaurids, *Palvennia hoybergeti* and *Sistertonia seeleyi* Fischer, Bardet, et al., 2014 (Delsett et al., 2018). However, in neither of these cases does the dorsal margin exhibit the distinctive arrowhead-like shape observed in *Eternauta*.

The region comprising the retroarticular process of the mandible in *Eternauta* shows very few similarities with other ophthalmosaurids. This process is strongly inclined posterodorsally and does not exhibit any medial curvature. In *Nannopterygius* the posterior portion of the surangular is ventrally curved (Zverkov & Jacobs, 2021), giving it a somewhat similar appearance to the condition observed in *Eternauta*. However, in the latter, this ventral curvature is absent. In remaining ophthalmosaurids this region of the mandible is mostly horizontally oriented (e.g. Barrientos-Lara & Alvarado-Ortega, 2021a; Delsett et al., 2018; Druckenmiller et al., 2012; Fischer et al., 2012), even in some of the earliest specimens like those recently recovered from the Bajocian of Luxembourg (Fischer et al., 2021). Among the more early-diverging parvipelvians, *Hauffiopteryx* spp. exhibit a similar curvature, though not immediately adjacent to the retroarticular process; rather, it occurs just below the orbit (Maxwell & Cortés 2020).

Aalenian records of marine reptiles, particularly ophthalmosaurid ichthyosaurs, are exceedingly rare and fragmentary (Druckenmiller & Maxwell, 2014; Fernández, 2003; Fischer et al., 2021). Consequently, comparisons of the forefin of *Eternauta* are limited to a single specimen (MLP-PV 92-III-2–1) that remains indeterminate at lower taxonomic levels (e.g. genus). Specimen MLP-PV 92-III-2–1 consists of the distal portion of a humerus, along with zeugopodial and mesopodial elements recovered from Aalenian levels of Los Molles Fm., Mendoza Province, Argentina (Fernández, 2003). The humerus is largely incomplete, preserving only the three distal articular facets for the zeugopodium, which are similar in proportion to those of *Eternauta*. However, aside from the pentagonal shape of the radius, the remaining zeugopodial elements differ markedly from those of *Eternauta*: both the aae and the ulna are rounded to oval in shape, whereas in *Eternauta*, the aae is droplet-shaped and the ulna is nearly rectangular.

With the exception of *P. hoybergeti*, *Arthropterygius* spp. and closely related taxa (*Janusaurus lundi* Roberts et al., 2014 and *Keilhauia nui*) exhibit a distinctive humeral morphology, characterised by a distal end slightly wider than the proximal, minimal midshaft constriction, and compression of the posterior third of the shaft (Campos et al., 2021). While *Eternauta* shares the first of these features, it does not exhibit additional similarities in humeral morphology with this clade of ophthalmosaurids (Figure 9).

Most ophthalmosaurids exhibit three distal articular facets on the humerus, being exceptions *N. enthekiodon*, *U.*? *kristiansenae*, *U.*? *kielanae* and *Sveltonectes insolitus* (Druckenmiller et al., 2012; Fischer et al., 2011; Moon & Kirton, 2018; Tyborowski, 2016). The most common condition, also observed in *Eternauta*, comprises facets for an anterior accessory element, the radius, and the ulna. This differs from forms that unambiguously possess a facet for the intermedium, such as *B. extremus*, *Ae. leptospondylus*, and *Parrasaurus yacahuitztli* (Bardet & Fernández, 2000; Barrientos-Lara & Alvarado-Ortega, 2021a; von Huene, 1922). The condition in *Eternauta* also differs from that of '*Pl*'. *americanus* (Nace, 1939), which, despite having three distal humeral facets, lacks a facet for aae; instead, the most posterior facet articulates with the pisiform (Maxwell & Kear, 2010). Additionally, *Eternauta* differs from taxa such as *Cat. gaspariniae* and '*Pl.*' *hercynicus* Kuhn, 1946, which exhibit four distal facets. In *Cat. gaspariniae*, these include

facets for the radius and ulna, as well as an anterior facet for the aae and a posterior facet for the most proximal element of a postaxial accessory digit. In '*Pl.*' *hercynicus*, the fourth facet articulates with the pisiform (Fernández et al., 2021; Kolb & Sander, 2009). Regarding the arrangement of articular facets, irrespective of their number, several taxa exhibit an ulnar facet with an articular surface facing posterodistally, often described as a *posteriorly deflected ulnar facet* (e.g. Delsett et al., 2017; Fernández, 1997; Maxwell, 2010; Moon & Kirton, 2016; Roberts et al., 2014). In *Eternauta*, this deflection is present and accompanied by a conspicuous ventral displacement of the ulnar facet – a feature otherwise documented in the holotype of *Arthropterygius chrisorum*, though in the latter, this displacement is far less pronounced (Maxwell, 2010).

At zeugopodial level, *Eternauta* differs from the majority of the Jurassic ophthalmosaurids in having a droplet-shaped aae with a pointed proximal apex in contact with the humerus and broad distal bulge, as *Undorosaurus*? *kristiansenae* (only in the right forefin) and *Su. argentina* (Campos et al., 2021; Druckenmiller et al., 2012). Other Late Jurassic taxa possess a similar aae, but in these cases this element is not in direct contact with humerus (e.g. Tyborowski, 2016; Moon & Kirton, 2018). Remaining ophthalmosaurids show an oval or square-shaped aae (e.g. Barrientos-Lara & Alvarado-Ortega, 2021a; Delsett et al., 2018; Roberts et al., 2014).

Palaeoecology of *Eternauta*

Currently, four valid ophthalmosaurid taxa are recognised from the Tithonian – Berriasian outcrops of the Vaca Muerta Fm.: *Cay. bonapartei*, *Ar. thalassonotus*, *Cat. gaspariniae*, and *Su. argentina* (Campos et al., 2020, 2021; Fernández, 1997; Fernández et al., 2021). The recognition of *Eternauta* as a new genus and species not only increases the taxonomic diversity of this lithostratigraphic unit but also broadens the range of inferred palaeoecological aspects among the ichthyosaurs that inhabited the southwestern margin of the Palaeo-Pacific towards the end of the Jurassic. In this context, two anatomical regions of *Eternauta*—the sclerotic ring and the posterior mandible – warrant particular attention due to their relevance in sensory and feeding performance.

Ocular dimensions exhibit a strong ecological signal: enlarged eyes – a trait particularly pronounced in ichthyosaurs – are consistent with adaptations to low-light pelagic environments, likely enhancing prey detection and predator avoidance (Fernández et al., 2005; Motani et al., 1999). Particularly, the aperture of the sclerotic ring has been widely used as an accurate proxy for the total amount of light a given system can receive and for visual acuity (Motani, 1999; Humphries & Ruxton, 2002; Fernández et al., 2005; Fischer, Arkhangelsky, et al., 2014). Among ichthyosaurs recovered from the Neuquén Basin, the maximum sclerotic aperture of *Eternauta* is about 10%-8% bigger than that of *Cay. bonapartei* and over 40% when compared with that of *Cat. gaspariniae*. Only in *Mollesaurus* from the Bajocian similar maximum sclerotic aperture is found (Supplementary Material, Table S1). The presence of a sclerotic ring almost completely filling the orbit has been interpreted either as a feature of immature individuals or as related to deep-diving habits (e.g. Fernández et al., 2005). However, the macro- and microanatomical characteristics of specimen MLP-PV 85-I-15–1 indicate that it was osteologically mature, suggesting that this condition in *Eternauta* is unlikely to reflect immaturity. Instead, it probably points to a visual system well adapted to exploiting different parts of the water column relative to other ophthalmosaurids inhabiting the Tithonian seas of the Vaca Muerta Formation.

The posterior region of the mandible in *Eternauta* exhibits a marked posterodorsal curvature, an unusual configuration among ophthalmosaurids. This morphology modifies the spatial relationship between the origin and insertion of two jaw muscles. The M. depressor mandibulae, responsible for jaw opening, originates from the occipital region and inserts on the retroarticular process. In *Eternauta*, the curvature of the posterior mandible shortens the linear distance between these two points, potentially reducing the torque and overall force transmitted by this muscle. However, this same geometry may increase the angular velocity of jaw opening, favouring rapid mandibular depression at the expense of power. In contrast, the M. adductor mandibularis internus pterygoideus, originating on the pterygoid flange and inserting on the angular, would experience an elongation of its fibre trajectory due to the posterodorsal displacement of the posterior mandible. This configuration likely enhances its role as a stabilising muscle, generating medially directed forces to maintain articulation between glenoid fossa and the quadrate condyle during jaw motion, as previously suggested for *Ichthyosaurus* (McGowan, 1973).

These anatomical interpretations align with the low jaw-opening mechanical advantage (OMA) calculated for *Eternauta* (Figure 12), which falls within the same range as *Hauffiopteryx typicus* and *Stenopterygius quadriscissus*. *Hauffiopteryx* has been interpreted as a fast but weak snap feeder, adapted to capturing small, soft-bodied prey (Jamison-Todd et al., 2022; Maxwell & Cortés, 2020), whereas gut content analyses

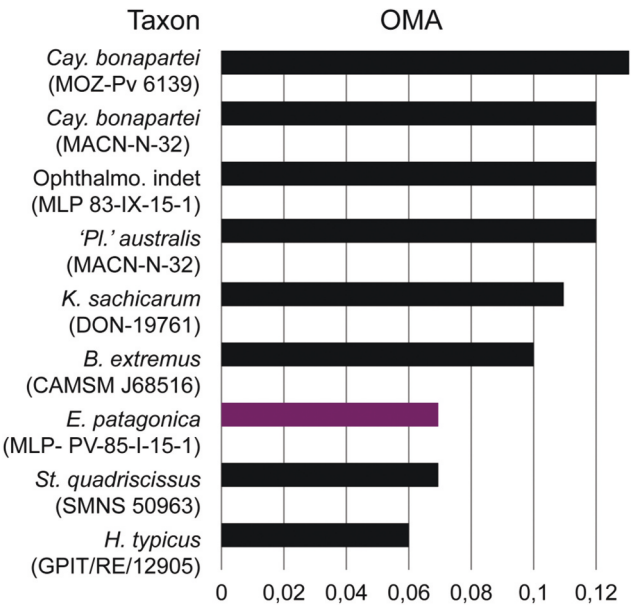

Figure 12. OMA values calculated for different parvipelvian taxa.

of adult *Stenopterygius quadriscissus* indicate a diet consisting exclusively of cephalopods (Dick et al., 2016). Notably, *Eternauta* also differs markedly in OMA from '*Pl. australis*', a presumed apex predator based on cranio-dental features and gut contents that include fish, turtles, and birds (Fischer et al., 2016; Kear et al., 2003). The inferred higher OMA of '*Pl. australis*' is consistent with a more forceful but slower jaw depression, suitable for seizing and subduing larger or more resistant prey. Similarly, *Kyhytysuka sachicarum*—a hypercarnivorous ophthalmosaurid with a robust snout, a strongly reinforced symphysis, and a horizontally oriented retroarticular process (Cortés et al., 2021) – and *Brachypterygius extremus*, which has also been recognized as an apex predator (Fischer et al., 2016), exhibit similarly high OMA values (based on CAMSM J68516) (Figure 12).

The comparison with *Cay. bonapartei* is particularly informative. This taxon has substantially higher OMA values (0.12–0.13), indicating a slower but more forceful jaw opening. This biomechanical disparity may reflect divergent prey preferences or feeding strategies within the same paleoenvironment. While *Eternauta* lacks the extreme rostral gracility of *Hauffiopteryx*, its low OMA and mandibular configuration suggest an emphasis on fast and precise jaw movement – potentially advantageous for capturing small, agile prey – rather than forceful biting. Taken together, the jaw morphology and ocular dimensions of *Eternauta* suggest a feeding strategy relying on relatively rapid but low-force jaw movements, potentially suited for capturing small or agile prey. While its sclerotic aperture is only marginally larger than that of *Cay. bonapartei*, it is substantially greater than in *Cat. gaspariniae*, reinforcing the idea that *Eternauta* occupied a somewhat distinct ecological role. The morphology and size of the tooth crowns is also congruent with a soft prey preference, as defined by Fischer et al. (2016).

The Tithonian seas of the Vaca Muerta Fm. hosted abundant nektonic prey such as ammonites (Vennari, 2016) as well as diverse fishes, including small- to medium-sized pachycormids like *Kaykay lafken* Gouiric-Cavalli & Arratia, 2021, aspidorhynchiforms, and caturids (Gouiric-Cavalli, 2016; Gouiric-Cavalli & Cione, 2015). Comparatively less diverse than ammonites, belemnites were also present and mainly represented by the genera *Belemnopsis* Bayle, 1878 and *Hibolithes* Montfort, 1808 (Vennari et al., 2023). These groups represent precisely the kind of small, agile prey that could have been targeted by a fast-jawed ichthyosaur such as *Eternauta*. These Tithonian seas also included large apex predators such as *Pliosaurus* Owen, 1842 and '*Dakosaurus*' *andiniensis* Vignaud & Gasparini, 1996 (Pol & Gasparini 2009; Gasparini & O'Gorman, 2014; O'Gorman et al., 2018), suggesting that at least some ophthalmosaurids may have relied on niche partitioning to avoid direct competition with these macropredators.

In this light, *Eternauta* can be interpreted as occupying a mesopredatory niche within the Tithonian seas of the Neuquén Basin, contrasting with both the apex predators (e.g. pliosaurids, metriorhynchids) and coeval ophthalmosaurids with higher OMA values (e.g. *Caypullisaurus*). This functional and ecological differentiation further underscores the role of niche partitioning in maintaining the high ichthyosaur taxonomic diversity recorded in the Vaca Muerta Fm. Moreover, these interpretations are in agreement with previous hypotheses on the trophic relationships of ichthyosaurs from the Neuquén Basin, particularly those from the Vaca Muerta Fm., which proposed that this lineage of marine reptiles belonged to a guild specializing in the active and sustained pursuit of agile prey (e.g. Fernández, 2007).

Conclusions

The re-examination of MLP-PV 85-I-15–1 reveals a distinctive combination of cranial and postcranial features that clearly differentiate it from *Caypullisaurus bonapartei*, to which it had previously been referred. In addition, the new taxon exhibits a unique set of traits – particularly in the postorbital region, palate and posterior mandible – that sets it apart from all other known ophthalmosaurids. Phylogenetic analysis places the new taxon within Platypterygiinae.

Its recognition also provides new insights into the extent of cranial morphological disparity within the clade, particularly in less-explored regions of the skull such as the palate. While each of the traits observed in the sclerotic ring, dentition and mandible of *Eternauta* occurs in other ichthyosaurs, their combined presence in this taxon supports a functional interpretation of specialisation on small, agile prey. This inferred trophic preference contributes to refining our understanding of ichthyosaur palaeoecology along the southwestern margin of Gondwana during Late Jurassic. Furthermore, the recognition of this new taxon highlights the Vaca Muerta Formation as one of the most taxonomically diverse ichthyosaur-bearing units globally, underscoring its significance for exploring and reconstructing Late Jurassic to Early Cretaceous marine faunas.

Acknowledgments

We thank Marcelo Reguero (MLP), Martín Ezcurra (MACN), Belén Bollini (MOZ), and Alberto Garrido (MOZ) for access to the collections under their care. Erin Maxwell and Feiko Miedema are warmly thanked for sharing images and data of *Argovisaurus*, and to Verónica Vennari and Soledad Gouiric-Cavalli for providing information and literature on the cephalopods and fishes of the Neuquén Basin, respectively. We also gratefully acknowledge the anonymous reviewers for their constructive comments, which greatly enhanced the quality of our work.

Disclosure statement

No potential conflict of interest was reported by the author(s).

Funding

This work was partially supported by the Agencia Nacional de Promoción Científica y Tecnológica PICT 2020-2067, CONICET PIP 2844, Programa de Incentivos Docentes UNLP-N981 and PI UNRN 40-A-1230.

ORCID

Lisandro Campos http://orcid.org/0000-0002-7201-8520
Marta S. Fernández http://orcid.org/0000-0001-6935-7575
Yanina Herrera http://orcid.org/0000-0002-2020-1227

Data availability statement

The data that support the findings of this study are openly available in Figshare at https://figshare.com/s/9d4b27d4e1cf54aacb9a.

References

Bardet, N. (1994). Extinction events among Mesozoic marine reptiles. *Historical Biology*, *7*(4), 313–324. https://doi.org/10.1080/10292389409380462

Bardet, N., & Fernández, M. S. (2000). A new ichthyosaur from the upper Jurassic lithographic limestones of Bavaria. *Journal of Paleontology*, *74*(3), 503–511. https://doi.org/10.1666/0022-3360(2000)074<0503:ANIFTU>2.0.CO;2

Barrientos-Lara, J. I., & Alvarado-Ortega, J. (2020). *Acuetzpalin carranzai* gen et sp. nov. A new ophthalmosauridae (Ichthyosauria) from the upper Jurassic of Durango, North Mexico. *Journal of South American Earth Sciences*, *98*, 102456. https://doi.org/10.1016/j.jsames.2019.102456

Barrientos-Lara, J. I., & Alvarado-Ortega, J. (2021a). A new Tithonian ophthalmosaurid ichthyosaur from Coahuila in northeastern Mexico. *Alcheringa: An Australasian Journal of Palaeontology*, *45*(2), 203–216. https://doi.org/10.1080/03115518.2021.1922755

Barrientos-Lara, J. I., & Alvarado-Ortega, J. (2021b). A new ophthalmosaurid (Ichthyosauria) from the upper kimmeridgian deposits of the La casita Formation, near Gómez Farías, Coahuila, Northern Mexico. *Journal of South American Earth Sciences*, *111*, 103499. https://doi.org/10.1016/j.jsames.2021.103499

Baur, G. (1887). Ueber den Ursprung der Extremitäten der Ichthyopterygia. *Jahresberichte und Mitteilungen des Oberrheinischen Geologischen Vereines*, *20*, 17–20.

Bayle, E. (1878). Atlas. Première partie. Fossiles principaux des terrains. *Explication de la Carte Géologique de la France, París*, *4*(part 1), 158.

Blainville, H. D. (1835). Description de quelques espèces de reptiles de la Californie, précédée de l'analyse d'un système général d'Erpétologie et d'Amphibiologie. *Nouvelles Annales du Muséum d'Histoire Naturelle*, *4*, 233–295.

Boulenger, G. A. (1904). On a new species of ichthyosaur from Bath. Proceedings of the Zoological Society of London, *1*, 424–426.

Campos, L., Fernández, M. S., Bosio, V., Herrera, Y., & Manzo, A. (2024). Revalidation of *myobradypterygius hauthali* Huene, 1927 and the phylogenetic signal within the ophthalmosaurid (Ichthyosauria) forefins. *Cretaceous Research*, *157*, 105818. https://doi.org/10.1016/j.cretres.2023.105818

Campos, L., Fernández, M. S., & Herrera, Y. (2020). A new ichthyosaur from the Late Jurassic of north-west Patagonia (Argentina) and its significance for the evolution of the narial complex of the ophthalmosaurids. *Zoological Journal of the Linnean Society*, *188*(1), 180–201. https://doi.org/10.1093/zoolinnean/zlz095

Campos, L., Fernandez, M. S., Herrera, Y., & Garrido, A. (2021). Morphological disparity in the evolution of the ophthalmosaurid forefin: New clues from the upper Jurassic of Argentina. *Papers in Palaeontology*, *7*(4), 1995–2020. https://doi.org/10.1002/spp2.1374

Chinsamy, A., & Raath, M. A. (1992). Preparation of fossil bone for histological examination. *Palaeontographia Africana*, *29*, 39–44.

Chinsamy-Turan, A. (2005). *The microstructure of dinosaur bone*. Johns Hopkins University Press. https://doi.org/10.56021/9780801881206

Cortés, D., Maxwell, E. E., & Larsson, H. C. (2021). Re-appearance of hypercarnivore ichthyosaurs in the Cretaceous with differentiated dentition: Revision of '*Platypterygius*' *sachicarum* (Reptilia: Ichthyosauria, Ophthalmosauridae) from Colombia. *Journal of Systematic Palaeontology*, *19*(14), 969–1002. https://doi.org/10.1080/14772019.2021.1989507

Delsett, L. L., Druckenmiller, P. S., Roberts, A. J., & Hurum, J. H. (2018). A new specimen of Palvennia hoybergeti: Implications for cranial and pectoral girdle anatomy in ophthalmosaurid ichthyosaurs. *PeerJ*, *6*, e5776. https://doi.org/10.7717/peerj.5776

Delsett, L. L., Roberts, A. J., Druckenmiller, P. S., & Hurum, J. H. (2017). A new ophthalmosaurid (Ichthyosauria) from Svalbard, Norway, and evolution of the ichthyopterygian pelvic girdle. *PLOS ONE*, *12*(1), e0169971. https://doi.org/10.1371/journal.pone.0169971

Dick, D. G., Schweigert, G., & Maxwell, E. E. (2016). Trophic niche ontogeny and palaeoecology of early Toarcian *Stenopterygius* (Reptilia: Ichthyosauria). *Palaeontology*, *59* (3), 423–431. https://doi.org/10.1111/pala.12232

Druckenmiller, P. S., Hurum, J. H., Knutsen, E. M., & Nakrem, H. A. (2012). Two new ophthalmosaurids (Reptilia: Ichthyosauria) from the Agardhfjellet Formation (upper Jurassic: Volgian/Tithonian), Svalbard, Norway. *Norwegian Journal of Geology/Norsk Geologisk Forening*, *92*, 311–339.

Druckenmiller, P. S., & Maxwell, E. E. (2010). A new lower Cretaceous (lower Albian) ichthyosaur genus from the Clearwater Formation, Alberta, Canada. *Canadian Journal of Earth Sciences*, *47*(8), 1037–1053. https://doi.org/10.1139/E10-028

Druckenmiller, P. S., & Maxwell, E. E. (2014). A middle Jurassic (Bajocian) ophthalmosaurid (Reptilia, Ichthyosauria) from the Tuxedni Formation, Alaska and the early diversification of the clade. *Geological Magazine*, *151*(1), 41–48. https://doi.org/10.1017/S0016756813000125

Ezcurra, M. D. (2024). Exploring the effects of weighting against homoplasy in genealogies of palaeontological phylogenetic matrices. *Cladistics*, *40*(3), 242–281. https://doi.org/10.1111/cla.12581

Fernández, M. S. (1997). A new ichthyosaur from the Tithonian (Late Jurassic) of the Neuquén Basin, northwestern Patagonia, Argentina. *Journal of Paleontology*, *71*(3), 479–484. https://doi.org/10.1017/S0022336000039494

Fernández, M. S. (1998). Nuevo material de *Caypullisaurus bonapartei* Fernández (reptilia: Ichthysauridae) del jurassico superior de la cuenca neuquina, Argentina. *Ameghiniana*, *35*, 21–24.

Fernández, M. S. (1999). A new ichthyosaur from the Los Molles formation (early Bajocian), Neuquén basin, Argentina. Journal of Paleontology, 73(4), 677–681.

Fernández, M. S. (2001). Dorsal or ventral? Homologies of the forefin of *caypullisaurus* (Ichthyosauria: Ophthalmosauria). *Journal of Vertebrate Paleontology*, *21*(3), 515–520. https://doi.org/10.1671/0272-4634(2001)021[0515:DOVHOT]2.0.CO;2

Fernández, M. S. (2003). Ophthalmosauria (Ichthyosauria) forefin from the Aalenian-Bajocian boundary of Mendoza province, Argentina. *Journal of Vertebrate Paleontology*, *23* (3), 691–694. https://doi.org/10.1671/1864

Fernández, M. S. (2007). Redescription and phylogenetic position of *caypullisaurus* (Ichthyosauria: Ophthalmosauridae). *Journal of Paleontology*, *81*(2), 368–375. https://doi.org/10.1666/0022-3360(2007)81[368:RAPPOC]2.0.CO;2

Fernández, M. S., Archuby, F., Talevi, M., & Ebner, R. (2005). Ichthyosaurian eyes: Paleobiological information content in the sclerotic ring of Caypullisaurus (Ichthyosauria, Ophthalmosauria). *Journal of Vertebrate Paleontology*, *25* (2), 330–337. https://doi.org/10.1671/0272-4634(2005)025[0330:IEPICI]2.0.CO;2

Fernández, M. S., Campos, L., Maxwell, E. E., & Garrido, A. C. (2021). *Catutosaurus gaspariniae*, gen. et sp. nov. (Ichthyosauria, Thunnosauria) of the upper Jurassic of Patagonia and the evolution of the ophthalmosaurids. *Journal of Vertebrate Paleontology*, *41*(1), e1922427. https://doi.org/10.1080/02724634.2021.1922427

Fernández, M. S., Herrera, Y., Vennari, V. V., Campos, L., De La Fuente, M., Talevi, M., & Aguirre-Urreta, B. (2019). Marine reptiles from the Jurassic/Cretaceous transition at the high Andes, Mendoza, Argentina. *Journal of South American Earth Sciences*, *92*, 658–673. https://doi.org/10.1016/j.jsames.2019.03.013

Fernández, M. S., & Talevi, M. (2014). Ophthalmosaurian (Ichthyosauria) records from the Aalenian–Bajocian of Patagonia (Argentina): An overview. *Geological Magazine*, *151*(1), 49–59. https://doi.org/10.1017/S0016756813000058

Fischer, V., Arkhangelsky, M. S., Uspensky, G. N., Stenshin, I. M., & Godefroit, P. (2014). A new lower Cretaceous ichthyosaur from Russia reveals skull shape conservatism within Ophthalmosaurinae. *Geological Magazine*, *151*(1), 60–70. https://doi.org/10.1017/S0016756812000994

Fischer, V., Bardet, N., Benson, R. B., Arkhangelsky, M. S., & Friedman, M. (2016). Extinction of fish-shaped marine reptiles associated with reduced evolutionary rates and global environmental volatility. *Nature Communications*, *7*(1), 10825. https://doi.org/10.1038/ncomms10825

Fischer, V., Bardet, N., Guiomar, M., & Godefroit, P. (2014). High diversity in Cretaceous ichthyosaurs from Europe prior to their extinction. *PLOS ONE*, *9*(1), e84709. https://doi.org/10.1371/journal.pone.0084709

Fischer, V., Maisch, M. W., Naish, D., Kosma, R., Liston, J. J., Joger, U., Krüger, F. J., Pérez, J. P., Tainsh, J. Y., & Appleby, R. M. (2012). New ophthalmosaurid ichthyosaurs from the European lower Cretaceous demonstrate extensive ichthyosaur survival across the Jurassic–Cretaceous boundary. *PLOS ONE*, *7*(1), e29234. https://doi.org/10.1371/journal.pone.0029234

Fischer, V., Masure, E., Arkhangelsky, M. S., & Godefroit, P. (2011). A new Barremian (early Cretaceous) ichthyosaur from western Russia. *Journal of Vertebrate Paleontology*, *31* (5), 1010–1025. https://doi.org/10.1080/02724634.2011.595464

Fischer, V., Weis, R., & Thuy, B. (2021). Refining the marine reptile turnover at the early–middle Jurassic transition. *PeerJ*, *9*, e10647. https://doi.org/10.7717/peerj.10647

Foffa, D., Young, M. T., & Brusatte, S. L. (2024). Comparative functional morphology indicates niche partitioning among sympatric marine reptiles. *Royal Society Open Science*, *11* (5), 231951. https://doi.org/10.1098/rsos.231951

Foffa, D., Young, M. T., Stubbs, T. L., Dexter, K. G., & Brusatte, S. L. (2018). The long-term ecology and evolution of marine reptiles in a Jurassic seaway. *Nature Ecology & Evolution*, *2*(10), 1548–1555. https://doi.org/10.1038/s41559-018-0656-6

Francillon-Vieillot, H., Buffrénil, V., de Castanet, J., Géraudie, J., Meunier, F. J., Sire, J. Y., Zylberberg, L., & Ricqlès, A. (1990). *Skeletal biomineralization: Patterns, processes and evolutionary trends: Microstructure and mineralization of vertebrate skeletal tissues*. Van Nostrand Reinhold.

Gasparini, Z., Fernández, M. S., De La Fuente, M., Herrera, Y., Codorniú, L., & Garrido, A. (2015). Reptiles from lithographic limestones of the Los Catutos Member (middle—upper Tithonian), Neuquén Province, Argentina: An essay on its taxonomic composition and preservation in an environmental and geographic context. *Ameghiniana*, *52*(1), 1–28. https://doi.org/10.5710/AMGH.14.08.2014.2738

Gasparini, Z., & Goñi, R. (1990). Los ictiosaurios jurásico-cretácicos de la Argentina. In V. Volkheimer (Ed.), *Bioestratigrafia de los sistemas regionales del Jurásico y Cretácico de America del Sur* (Comité Sudamericano del Jurásico y Cretácico) (pp. 299–311).

Gasparini, Z., & O'Gorman, J. P. (2014). A new species of *pliosaurus* (sauropterygia, Plesiosauria) from the upper Jurassic of northwestern Patagonia, Argentina. *Ameghiniana*, *51*(4), 269–283. https://doi.org/10.5710/AMGH.03.04.2014.2225

Gilmore, C. W. (1906). Osteology of *Baptanodon* (Marsh). *Memoirs of the Carnegie Museum*, *2*(2), 77–128. https://doi.org/10.5962/p.234823

Goloboff, P. A., & Catalano, S. A. (2016). Tnt version 1.5, including a full implementation of phylogenetic morphometrics. *Cladistics*, *32*(3), 221–238. https://doi.org/10.1111/cla.12160

Gouiric-Cavalli, S. (2016). A new late Jurassic halecomorph fish from the marine Vaca Muerta Formation, Argentina, southwestern Gondwana. *Fossil Record*, *19*(2), 119–129. https://doi.org/10.5194/fr-19-119-2016

Gouiric-Cavalli, S., & Arratia, G. (2021). A new† pachycormiformes (actinopterygii) from the upper Jurassic of Gondwana sheds light on the evolutionary history of the group. *Journal of Systematic Palaeontology*, *19*(21), 1517–1550. https://doi.org/10.1080/14772019.2022.2049382

Gouiric-Cavalli, S., & Cione, A. L. (2015). Fish faunas from the Late Jurassic (Tithonian) Vaca Muerta Formation of Argentina: One of the most important Jurassic marine ichthyofaunas of Gondwana. *Journal of South American Earth Sciences*, *63*, 114–124. https://doi.org/10.1016/j.jsames.2015.07.002

Herrera, Y., Fernández, M. S., & Vennari, V. V. (2021). *Cricosaurus* (thalattosuchia, metriorhynchidae) survival across the J/K boundary in the high Andes (Mendoza Province, Argentina). *Cretaceous Research*, *118*, 104673. https://doi.org/10.1016/j.cretres.2020.104673

Hulke, J. W. (1871). Note on an *Ichthyosaurus* (*I. enthekiodon*) from Kimmeridge Bay, Dorset. *The Quarterly Journal of the Geological Society of London*, *27*(1–2), 440–441. https://doi.org/10.1144/GSL.JGS.1871.027.01-02.52

Humphries, S., & Ruxton, G. D. (2002). Why did some ichthyosaurs have such large eyes? *Journal of Experimental Biology*, *205*(4), 439–441. https://doi.org/10.1242/jeb.205.4.439

Jacobs, M. L., & Martill, D. M. (2020). A new ophthalmosaurid ichthyosaur from the upper Jurassic (early Tithonian) Kimmeridge Clay of Dorset, UK, with implications for Late Jurassic ichthyosaur diversity. *PLOS ONE*, *15*(12), e0241700. https://doi.org/10.1371/journal.pone.0241700

Jamison-Todd, S., Moon, B. C., Rowe, A. J., Williams, M., & Benton, M. J. (2022). Dietary niche partitioning in early Jurassic ichthyosaurs from Strawberry Bank. *Journal of Anatomy*, *241*(6), 1409–1423. https://doi.org/10.1111/joa.13744

Kear, B. P. (2005). Cranial morphology of *Platypterygius longmani* Wade, 1990 (Reptilia: Ichthyosauria) from the lower Cretaceous of Australia. *Zoological Journal of the Linnean Society*, *145*(4), 583–622. https://doi.org/10.1111/j.1096-3642.2005.00199.x

Kear, B. P., Boles, W. E., & Smith, E. T. (2003). Unusual gut contents in a Cretaceous ichthyosaur. *Proceedings of the Royal Society of London, Series B: Biological Sciences*, *270*(suppl_2), 206–208. https://doi.org/10.1098/rsbl.2003.0050

Kear, B. P., Engelschiøn, V. S., Hammer, Ø., Roberts, A. J., & Hurum, J. H. (2023). Earliest Triassic ichthyosaur fossils push back oceanic reptile origins. Current Biology, 33(5), R178–R179.

Kolb, C., & Sander, P. M. (2009). Redescription of the ichthyosaur *platypterygius hercynicus* (Kuhn 1946) from the Lower Cretaceous of Salzgitter (Lower Saxony, Germany). *Palaeontographica Abteilung A: Paläozoologie*, *288*(4–6), 151–192. https://doi.org/10.1127/pala/288/2009/151

Kuhn, O. (1946). Ein skelett von *ichthyosaurus hercynicus* n. sp. aus dem Aptien von Gitter. *Berichte der Naturforschenden Gesellschaft Bamberg*, *29*, 69–82.

MacLaren, J. A., Anderson, P. S., Barrett, P. M., & Rayfield, E. J. (2017). Herbivorous dinosaur jaw disparity and its relationship to extrinsic evolutionary drivers. *Paleobiology*, *43*(1), 15–33. https://doi.org/10.1017/pab.2016.31

Maddison, W. P., & Maddison, D. R. (2019). Mesquite: A modular system for evolutionary analysis, version 3.61. http://www.mesquiteproject.org

Marsh, O. C. (1879). A new order of extinct reptiles (Sauranodonta) from the Jurassic formation of the Rocky Mountains. *The American Journal of Science*, *3*(17), 85–86. https://doi.org/10.2475/ajs.s3-17.97.85

Massare, J. A. (1988). Swimming capabilities of Mesozoic marine reptiles: Implications for method of predation. *Paleobiology*, *14*(2), 187–205. https://doi.org/10.1017/S009483730001191X

Maxwell, E. E. (2010). Generic reassignment of an ichthyosaur from the Queen Elizabeth Islands, Northwest Territories, Canada. *Journal of Vertebrate Paleontology*, *30*(2), 403–415. https://doi.org/10.1080/02724631003617944

Maxwell, E. E., & Caldwell, M. W. (2006). A new genus of ichthyosaur from the lower Cretaceous of western Canada. *Palaeontology*, *49*(5), 1043–1052. https://doi.org/10.1111/j.1475-4983.2006.00589.x

Maxwell, E. E., & Cortés, D. (2020). A revision of the early Jurassic ichthyosaur Hauffiopteryx (Reptilia: Ichthyosauria), and description of a new species from

southwestern Germany. *Palaeontologia Electronica*, *23*, 1–43. https://doi.org/10.26879/937

Maxwell, E. E., & Kear, B. P. (2010). Postcranial anatomy of *platypterygius americanus* (Reptilia: Ichthyosauria) from the Cretaceous of Wyoming. *Journal of Vertebrate Paleontology*, *30*(4), 1059–1068. https://doi.org/10.1080/02724634.2010.483546

McGowan, C. (1973). The cranial morphology of the lower Liassic latipinnate ichthyosaurs of England. *Bulletin of the British Museum (Natural History) Geology*, *24*(1), 1–109. https://doi.org/10.5962/p.313822

McGowan, C., & Motani, R. (2003). *Handbook of paleoherpetology: Part 8 ichthyopterygia*. Verlag Dr. Friedrich Pfeil.

M'Coy, F. L. (1867). On the occurrence of *ichthyosaurus* and *plesiosaurus* in Australia. *The Annals and Magazine of Natural History*, *19*(113), 355–356. https://doi.org/10.1080/00222936708562678

Miedema, F., Bastiaans, D., Scheyer, T. M., Klug, C., & Maxwell, E. E. (2024). A large new Middle Jurassic ichthyosaur shows the importance of body size evolution in the origin of the Ophthalmosauria. *BMC Ecology and Evolution*, *24*(1), 34. https://doi.org/10.1186/s12862-024-02208-3

Miedema, F., & Maxwell, E. E. (2022). Ontogenetic variation in the skull of *Stenopterygius quadriscissus* with an emphasis on prenatal development. *Scientific Reports*, *12*(1), 1707. https://doi.org/10.1038/s41598-022-05540-0

Montfort D. Tome I. Chez F. Schoell (Eds). (1808). *Conchyliologie systématique et classification méthodique des coquilles. Coquilles univalves, cloisonnees*, (p. 410). F. Schœll.

Moon, B. C., & Kirton, A. M. (2016). Ichthyosaurs of the British Middle and upper Jurassic part 1, *ophthalmosaurus*. *Monographs of the Palaeontographical Society*, *170*(647), 1–84. https://doi.org/10.1080/02693445.2016.11963958

Moon, B. C., & Kirton, A. M. (2018). Ichthyosaurs of the British middle and upper Jurassic. Part 2. *Brachypterygius, Nannopterygius, Macropterygius and Taxa Invalida*. *Monographs of the Palaeontographical Society*, *172*(650), 85–177. https://doi.org/10.1080/02693445.2018.1468139

Motani, R. (1999). Phylogeny of the ichthyopterygia. *Journal of Vertebrate Paleontology*, *19*(3), 473–496. https://doi.org/10.1080/02724634.1999.10011160

Motani, R. (2005). Evolution of fish-shaped reptiles (Reptilia: Ichthyopterygia) in their physical environments and constraints. *Annual Review of Earth and Planetary Sciences*, *33*(1), 395–420. https://doi.org/10.1146/annurev.earth.33.092203.122707

Motani, R., Rothschild, B. M., & Wahl, W., Jr. (1999). Large eyeballs in diving ichthyosaurs. *Nature*, *402*(6763), 747–747. https://doi.org/10.1038/45435/

Nace, R. L. (1939). A new ichthyosaur from the upper Cretaceous Mowry Formation of Wyoming. *The American Journal of Science*, *237*(9), 673–686. https://doi.org/10.2475/ajs.237.9.673

Ochev, V. G., & Efimov, V. M. (1985). A new genus of ichthyosaur from the Ul'yanovsk area of the Povolzh'ye region. *Paleontological Journal*, *4*, 87–91.

O'Gorman, J. P., Gasparini, Z., & Spalletti, L. A. (2018). A new pliosaurus species (sauropterygia, Plesiosauria) from the upper Jurassic of Patagonia: New insights on the Tithonian morphological disparity of mandibular symphyseal morphology. *Journal of Paleontology*, *92*(2), 240–253. https://doi.org/10.1017/jpa.2017.82

Owen, R. (1842). Report on British fossil reptiles. Part II. *Reports of the British Association for the Advancement of Science*, *11*, 60–204.

Paparella, I., Maxwell, E. E., Cipriani, A., Roncace, S., & Caldwell, M. W. (2017). The first ophthalmosaurid ichthyosaur from the upper Jurassic of the Umbrian–Marchean Apennines (Marche, central Italy). *Geological Magazine*, *154*(4), 837–858. https://doi.org/10.1017/S0016756816000455

Páramo-Fonseca, M. E. (1997). *Platypterygius sachicarum* (Reptilia, Ichthyosauria) nueva especie del Cretácico de Colombia. *Revista Ingeominas*, *6*, 1–12.

Páramo-Fonseca, M. E., Cabra, C. D. B., & Camacho, R. G. (2024). A new species of *platypterygius* (Ophthalmosauridae) from the lower Barremian of Colombia and assessment of the species composition of the genus. *Earth Sciences Research Journal*, *28*(2), 103. https://doi.org/10.15446/esrj.v28n2.112332

Pardo-Pérez, J., Zambrano, P., Malkowski, M., Lomax, D., Villa-Martínez, R., Stinnesbeck, W., Frey, E., Scapini, F., Gasco, C., & Maxwell, E. E. (2024). Validity of *myobradypterygius hauthali* von Huene, 1927 (Ichthyosauria: Ophthalmosauria) from the early Cretaceous of Chile and Argentina. *Zoological Journal of the Linnean Society*, *202*(2), zlae106. https://doi.org/10.1093/zoolinnean/zlae106

Pol, D., & Escapa, I. H. (2009). Unstable taxa in cladistic analysis: Identification and the assessment of relevant characters. *Cladistics*, *25*(5), 515–527. https://doi.org/10.1111/j.1096-0031.2009.00258.x

Pol, D., & Gasparini, Z. (2009). Skull anatomy of *Dakosaurus andiniensis* (thalattosuchia: Crocodylomorpha) and the phylogenetic position of thalattosuchia. *Journal of Systematic Palaeontology*, *7*(2), 163–197. https://doi.org/10.1017/S1477201908002605

Ponstein, J., Hermanson, G., Jansen, M. W., Renaudie, J., Fröbisch, J., & Evers, S. W. (2024). Functional and character disparity are decoupled in turtle mandibles. *Ecology and Evolution*, *14*(11), e70557. https://doi.org/10.1002/ece3.70557

Quenstedt, F. A. (1856). *Der jura* (p. 842). H. Laupp.

Roberts, A. J., Druckenmiller, P. S., Sætre, G. P., & Hurum, J. H. (2014). A new upper Jurassic ophthalmosaurid ichthyosaur from the Slottsmøya Member, Agardhfjellet Formation of central Spitsbergen. *PLOS ONE*, *9*(8), e103152. https://doi.org/10.1371/journal.pone.0103152

Seeley, H. G. (1874). On the pectoral arch and fore limb of *Ophthalmosaurus*, a new ichthyosaurian genus from the Oxford clay. *Quarterly Journal of the Geological Society*, *30*(1–4), 696–707. https://doi.org/10.1144/GSL.JGS.1874.030.01-04.64

Talevi, M., Campos, L., & Fernández, M. S. (2021). Microanatomy and histology of the distal limb elements of ophthalmosaurids from the Middle Jurassic to the lower

Cretaceous of the Neuquén Basin, Patagonia, Argentina. *Cretaceous Research*, *121*, 104737. https://doi.org/10.1016/j.cretres.2020.104737

Talevi, M., Fernández, M. S., & Salgado, L. (2012). Variación ontogenética en la histología ósea de *Caypullisaurus bonapartei* Fernández, 1997 (Ichthyosauria: Ophthalmosauridae). *Ameghiniana*, *49*(1), 38–46. https://doi.org/10.5710/AMGH.v49i1(403)

Tyborowski, D. (2016). A new ophthalmosaurid ichthyosaur from the Late Jurassic of Owadów-Brzezinki quarry, Poland. *Acta Palaeontologica Polonica*, *61*(4), 791–803. https://doi.org/10.4202/app.00252.2016

Vennari, V. V. (2016). Tithonian ammonoids (Cephalopoda, Ammonoidea) from the Vaca Muerta Formation, Neuquén basin, west-central Argentina. *Palaeontographica, Abteilung A*, *85*(1–6), –165. https://doi.org/10.1127/pala/306/2016/85

Vennari, V. V., Aguirre-Urreta, B., Marin, L. S., Pellenard, P., Martínez, M., & Tunik, M. (2023). Upper Jurassic (Tithonian) belemnites from the Neuquén basin, Argentina. *Journal of South American Earth Sciences*, *124*, 104200. https://doi.org/10.1016/j.jsames.2023.104200

Vignaud, P., & Gasparini, Z. (1996). New *dakosaurus* (crocodylomorpha, Thalattosuchia) from the upper Jurassic of Argentina. *Comptes Rendus de l'Académie des Sciences*, *322*, 245–250.

von Huene, F. R. F. (1922). *Die ichthyosaurier des Lias und ihre zusammenhänge*. Verlag von gebrüder Borntraeger.

von Huene, F. R. F. (1931). Neue studien über ichthyosaurier aus Holzmaden. *Abhandlungen der Senckenbergischen Naturforschenden Gesellschaft*, *42*, 345–382.

Westneat, M. W. (1994). Transmission of force and velocity in the feeding mechanisms of labrid fishes (Teleostei, Perciformes). *Zoomorphology*, *114*(2), 103–118. https://doi.org/10.1007/BF00396643

Zverkov, N. G., & Efimov, V. M. (2019). Revision of *Undorosaurus*, a mysterious Late Jurassic ichthyosaur of the boreal realm. *Journal of Systematic Palaeontology*, *17*(14), 1183–1213. https://doi.org/10.1080/14772019.2018.1515793

Zverkov, N. G., & Jacobs, M. L. (2021). Revision of *nannopterygius* (Ichthyosauria: Ophthalmosauridae): Reappraisal of the 'inaccessible' holotype resolves a taxonomic tangle and reveals an obscure ophthalmosaurid lineage with a wide distribution. *Zoological Journal of the Linnean Society*, *191*(1), 228–275. https://doi.org/10.1093/zoolinnean/zlaa028